Nutrient Perturbation Drives Carbon Cycling in a Tropical Mangrove Estuary: The Wouri Estuary Douala, Cameroon

By

SUNJO CLARIS NYUYSONI

THESIS

Submitted in partial satisfaction of the requirements for the degree of

MASTER OF SCIENCE

in

Earth and Planetary Science

in the

OFFICE OF GRADUATE STUDIES

of the

UNIVERSITY OF CALIFORNIA

DAVIS

Approved:

Eliot A. Atekwana, Chair

Dawn Sumner

Alyssa J. Griffin

Committee in Charge

2024

Table of Contents

Acknowledgments

My heartfelt gratitude goes to my thesis advisor, Dr. Eliot Atekwana for his wonderful mentorship, support, and guidance throughout my research. It was indeed an honor to have experienced the dedication he put in to support me realize this project. I thank my thesis committee members Dr. Dawn Sumner and Dr. Alyssa Griffin for their support and constructive feedback during my academic journey. I extend immense thanks to my mentors Dean Estella Atekwana and Dr. Henry Agbogun for their intellectual and moral support. Much love and thanks to my family, especially my husband and kids for their sacrifice and for their daily words of encouragement.

I thank the government of Cameroon (Ministry of Water Resources and Energy) for granting me research permits to conduct this research in the Douala Estuary, Cameroon. I thank the manager and staff of the L'Aquarius Marina 2000 Hotel for providing me with sample processing space and other logistics which facilitated my field work. This work would not have been possible without the contributions of the field team. I thank the students participating in the US National Science Foundation International Experience for Students 2023 field season for helping with sampling and data acquisition. I thank the boat drivers (Emmanuel Lepanye Jackson, Salvation Benson, and Tecno) for cruising with me and making this work possible. Above all, I return all glory to God Almighty for leading me through this journey. This Thesis is dedicated to All students in the Northwest and Southwest regions of Cameroon who have been stripped of their right to quality education.

This thesis is an original work written by me under the supervision of Dr. Eliot Atekwana and with the approval of my thesis committee. The work has not been published in any format anywhere.

Highlights

- Salinity-$\delta^{18}O$ relationship reveals two-endmember hydrologic mixing in a tropical mangrove estuary
- Hydrologic mixing does not control the distribution of anthropogenic nitrates
- Anthropogenic nitrate perturbation is in situ, and not from a seawater or freshwater source
- Hydrologic mixing accounts for the distribution of alkalinity and dissolved inorganic carbon
- Nitrate pollution fuels CO_2 generation that causes the $\delta^{13}C$ to deviate from conservative mixing

Keywords: Dissolved inorganic carbon; Stable carbon isotopes; Stable oxygen isotopes; Dissolved silica; Nitrate pollution; Cameroon

Abstract

I investigated water temperature, dissolved oxygen (DO), clarity, salinity, stable oxygen isotopes ($\delta^{18}O$), pH, alkalinity, dissolved inorganic carbon (DIC), the stable carbon isotope of DIC ($\delta^{13}C_{DIC}$), silica, and nitrate in the open water of a tropical mangrove estuary and rivers feeding the estuary. I aimed to document how anthropogenic pollution by nutrients drives carbon cycling in the open water of the estuary. Salinity-$\delta^{18}O$ mixing modeling confirmed a two-endmember seawater-freshwater hydrologic mixing in the estuary. The spatial distribution of alkalinity and DIC was modeled by a two-endmember seawater-freshwater mixing. However, a salinity-DIC-$\delta^{13}C_{DIC}$ conservative mixing model revealed a mismatch in stations in the lower estuary because of isotopically lower-than-expected $\delta^{13}C_{DIC}$. I attribute the isotopically lower than predicted $\delta^{13}C_{DIC}$ to nitrate-driven eutrophication and subsequent production of isotopically light CO_2 from organic matter oxidation. The anthropogenic nitrate perturbation that drives the cycling of carbon near the mouth of this tropical estuary is not sourced from seawater or freshwater but generated in situ. My findings implicate anthropogenic pollution from shipping activities in the carbon cycling in this tropical mangrove estuary.

1. Introduction

Estuaries amongst other coastal habitats are considered critical ecosystems and are known for their abundant biodiversity and high bioproductivity. Estuaries receive significant amounts of organic carbon from land which is processed and exchanged with the ocean and atmosphere (Giresse and Cahet 1997; Borges and Abril 2011; Chen et al. 2013; de Souza Machado 2017; Dutta and Choudhury 2021). A recent estimate of global estuarine CO_2 degassing to the atmosphere is ~0.1 pgC yr^{-1} (Chen et al. 2013), making estuaries an important interface in the conversion of terrestrial and coastal carbon, and their transfer to the atmospheric and oceanic reservoirs (Frankignoulle et al.1998; Abril et al. 2005; Borges et al. 2005; Chen et al. 2012; Houang et al. 2012). Globally, about 60% of estuarine systems are changing in response to anthropogenic forcing (Bouillon et al. 2003; Borges 2005). Altered freshwater inflows and increased nutrient loading from watersheds of rivers that discharge to estuaries affect estuary productivity and nutrient and carbon cycling (Fry 2002; Atekwana et al. 2003; Gazeau et al. 2004; Abril 2011; Chen et al. 2013; Dutta and Choudhury 2021). Estuaries are therefore critical areas for research on carbon sources, sinks, and fluxes, as estuaries link the terrestrial, ocean, and atmospheric carbon reservoirs.

Understanding the processes that control the occurrence, distribution, and processing of geogenic solutes and nutrients is critical to elucidating their role as tracers and drivers, respectively, of carbon cycling in estuaries (Stumn and Morgan 1993; Fry 2002; Atekwana et al. 2003). In estuaries, the salinity-$\delta^{18}O$ relationship is used to trace mixing between seawater and freshwater, because salinity and $\delta^{18}O$ are conservative, and seawater and freshwater endmembers are well-defined. (Eyre 1999; Fry 2002). Therefore, the relationship between salinity and solutes, nutrients, and dissolved inorganic carbon (DIC) can be used to assess whether their spatial and temporal distribution in the water column in estuaries is from the mixing of river and seawater sources or

water column production (Strain and Tan 1979; Loder 1985; Dubinina et al. 2017; Joesoef et al. 2017). The stable carbon isotope ratio of DIC ($\delta^{13}C_{DIC}$) is also useful for determining marine and terrestrial contributions to the estuarine DIC pool and for carbon cycling. Nutrient perturbations (e.g., nitrate) can fuel increased productivity in the water column and promote eutrophication leading to a drawdown of water column dissolved oxygen (hypoxia) (Borges and Gypens 2010; Zhang et al. 2019; Cotovicz 2019, 2021; Dutta and Choudhury 2021; Hee et al. 2023). Furthermore, heterotrophic and photosynthetic processes control the behavior of $\delta^{13}C_{DIC}$ in the aqueous DIC pool in estuaries by adding or removing carbon from the DIC pool (Bouillon et al. 2003, 2011). Therefore, the conservative and nonconservative mixing models based on salinity, DIC, and the $\delta^{13}C_{DIC}$ provide a basis for assessing and understanding the cycling of carbon in estuaries (Strain and Tan 1979; Peterson et al. 1994; Hellings et al. 1999; Atekwana et al. 2003).

Tropical mangrove estuaries are an integral part of global carbon and nutrient cycling (Twilley, 1985; Dittmar and Lara 2001; Bouillon et al. 2007; Donato et al. 2011; Palit et al. 2022). Estimates show that ~21% of the World's mangroves are in Africa, with 74% occupying the coastlines of tropical west Africa and 26% occupying the tropical east coast of Africa (Naidoo 2023; Diop 1992, 1993; Diop et al. 2002). Although tropical estuaries in sub-Saharan Africa harbor ~31% of the human population and receive far greater amounts of organic and inorganic carbon and pollutants compared to temperate estuaries (Diop 1993; Diop et al. 2002, 2014; Anjonina 2008; Naidoo 2023) tropical mangrove estuaries in sub-Saharan Africa have not been investigated for their role in local, regional, or even global carbon cycling. It is unclear what factors control carbon cycling in the open waters of tropical mangrove estuaries. Published investigations conducted in tropical mangrove estuaries in sub-Saharan Africa are focused on point source pollution, mangrove mapping, coastline evolution, and hydrodynamics (e.g., Diop 1993; Diop et al. 2002, 2014;

Corcoran et al 2007; Anjonina 2008; Naidoo 2023). There is a gap in our knowledge and understanding of the role of watersheds in delivering anthropogenic nutrients that drive biogeochemical processes that cycle carbon in the open water of tropical mangrove estuaries.

In this study, I investigated the role of nutrients from anthropogenic pollution in upsetting the carbon cycling in the open water of the tropical mangrove Wouri Estuary, Douala, Cameroon (Fig. 1). The Wouri Estuary is a complex and extensive mangrove ecosystem which is a critical habitat for biodiversity that supports the fishing industry in Cameroon. Recent studies have shown that seawater-freshwater hydrologic mixing in the mouth of rivers and tidal creeks is definable from tide-salinity relationships (Atekwana et al. 2022, Fotsi et al. 2023). An investigation of the Wouri Estuary and Rio Del Ray Estuary along the Cameroon coastline by Gabche and Smith (2002) suggests that anthropogenic activities in river watersheds pollute the Wouri Estuary. The sources of pollution in the Wouri Estuary include industries located at the head of the estuary and the mouth of the Wouri River (Gabche and Smith 2002; Atangana 2013; Ngoran 2016; Mbusnum et al. 2020). Although previous studies have revealed that the Wouri Estuary is polluted, there are no studies that assess the effect of such pollution on carbon cycling in the estuary. Thus, my goal in this study was to conduct a chemical and isotopic survey of the Wouri Estuary and the major rivers (Wouri River, Mungo River, and Dibamba River) that feed the estuary to assess if and how anthropogenic pollution (e.g., nitrate) perturbs the estuarine carbon cycle. The investigation was conducted during the peak of the rainy season (July) when the annual river discharge into the estuary is highest, and consequently, more pollutants from the watershed are washed into the estuary. To achieve my goal, I conducted an axial survey of water temperature, dissolved oxygen (DO), clarity, salinity, $\delta^{18}O$, pH, alkalinity, DIC, $\delta^{13}C_{DIC}$, silica, and nitrate in the open water of the Wouri Estuary and the rivers that feed the estuary. I found out that: (1) seawater-freshwater hydrologic mixing controls

the distribution of DIC and geogenic solutes, but not anthropogenic nitrate and (2) anthropogenic nitrate perturbation of the cycling of carbon in the Wouri Estuary occurs near the estuary mouth and is not associated freshwater or oceanic sources. My findings are used to suggest that anthropogenic nutrient impacts from shipping activities drive carbon cycling near the mouth of the tropical Wouri Estuary.

2. Study area

The Wouri Estuary (3°42′0.00″N to 4°11′0.00″N and 9°14′.00″E to 9°35′0.00″E) is located in Douala, Cameroon, along the Atlantic coast of West Africa (Fig. 1). The Wouri Estuary has a low-lying relief that varies between sea level and ~3 m above sea level (a.s.l) to the west and ~100 m a.s.l in the northeast (Gabche and Smith 2002; Ndongo et al. 2015; Fotsi et al. 2019; Simon and Raffaeli 2012; Besack et al. 2021). The Wouri Estuary has open water of approximately 1485 km^2 and is surrounded by 2300 to 2700 km^2 of mangrove forest (Gabche and Smith 2002; Din et al. 2008, 2017; Simon and Raffaeli 2012; Ndongo et al. 2015; Fotsi et al. 2019). The mangrove forest is composed of more than 30 species, with the red mangroves [Rhizophora racemose; Rhizophora harrisonii; Rhizophora mangle (Phizophoraceae) and white mangroves (cennia germnans (Avicenniaceae); Laguncularia racemose) and conocarpus erectus) as the dominant species (Din 2001; Din et al. 2002, 2008; Din and Baltzer 2008; Nfotabong-Atheull et al. 2011, 2013; Fantong et al. 2016; Fusi et al. 2016).

The open water of the Wouri Estuary extends from the Atlantic coast to ~35 km inland and has a width that varies from 23 km in the lower estuary to 1.2 km at the estuary head. The Douala seaport is located near the head of the Wouri Estuary. The Douala seaport serves landlocked countries of the Sub-Saharan Africa region (Mbusnum et al. 2020). Because of the large volume of sediment delivered by the Wouri River, Mungo River and Dibamba River to the estuary, a shipping channel

from the Atlantic Ocean to the port is periodically dredged and maintained to facilitate ship navigation. The maximum depth of the navigable channel after dredging is 25 m which decreases to 6 m around the Bonaberi bridge at the estuary head (Gabche and Smith 2002; Simon and Raffaeli 2012; Ndongo et al. 2015; Fotsi et al. 2019; Besack et al. 2021). Also, the number of ships that can offload cargo usually exceeds the port's holding capacity. Therefore, ships in transit to the port wait near the estuary mouth for their turn to pick up or offload cargo.

The climate of Wouri Estuary and the coastal region is classified as a warm humid equatorial regime (Peel et al. 2007; Din and Baltzer 2008), with distinct dry and rainy seasons (Din et al. 2002; Fantong et al. 2016; Mbusnum et al. 2020; Climate-Data.org 2023). The dry season spans December to February and the rainy season spans March to November. The daily temperature ranges between 23 and 33 ^{0}C and is between 25 and 33 ^{0}C in the dry season and 21 and 29 ^{0}C in the rainy season. The annual average temperature is 26.4 ^{0}C. The average annual precipitation is 4000 cm and distributed such that ~75% of the rain falls in the rainy season (Gabche and Smith 2002; Din et al. 2002; Climate-Data.org 2023). The highest monthly rainfall recorded within the year occurs in June, July, and August. During the dry season, the Harmattan winds blow from the Sahara Desert in the north, causing low humidity (as low as 48%) and high temperature; while during the rainy season, the moisture-laden winds blow from the Gulf of Guinea in the south causing high humidity. Humidity approaching an absolute maximum of 100 % during the rainy season is typical of this region (Din et al. 2002; Weather-forecast.com/Cameroon).

The hydrology of the Wouri Estuary is supported by the Wouri River, Mungo River, and Dibamba River (Fig. 1) (Gabche and Smith 2002; Fantong et al. 2016; Ramatlapeng et al. 2021; Ndondo et al. 2021; Atekwana et al. 2022). The Wouri River enters the estuary at its head, and the Mungo River flows into the estuary from the west and the Dibamba River flows into the estuary from the

east about 15 km from the estuary mouth. The Wouri River has a catchment of ~8250 km^2 and discharges 40 x 10^6 m^3/d into the Wouri Estuary (Gabche and Smith 2002). The Wouri River and its tributaries drain the volcanic rocks of the Western High Plateau in the west region and sedimentary rocks of the Littoral region (Gabche and Smith 2002; Fantong et al. 2016; Fomenky et al. 2019; Besack et al. 2021). Although a large portion of the Wouri River watershed is rural, the river flows through the city of Douala with a population of ~8 million (Olivry 1986; Gabche and Smith 2002; Ako et al. 2014). The Mungo River has a catchment of 4200 km^2 and discharges 60 x 10^6 m^3/d into the Wouri Estuary (Gabche and Smith 2002). The Mungo River and its tributaries drain the volcanic outpours of Mt. Cameroon. Additionally, the Mungo River and its tributaries flow through agricultural areas with plantations, as well as semi-urban and urban areas where population density reaches up to 150 inhabitants/km^2 (Ako et al. 2014; Olivry 1986; Gabche and Smith 2002). River runoff into the estuary from the Dibamba River is 40 x 10^6 m^3/d from a catchment of ~2400 km^2 (Gabche and Smith 2002). The Dibamba River and its tributaries drain metamorphic rocks of the Nyong complex (Besack et al. 2021, Fantong et al. 2017; Gabche and Smith 2002). The watershed is rural; however, the river flows briefly through the eastern portion of the city of Douala.

The Wouri Estuary experiences semidiurnal mixed tides with tidal ranges changing from mesotidal (>2 m) to microtidal (<2 m) (Onguene et al. 2014). During one tidal cycle, the tidal wave can propagate more than 60 km upstream from the estuary mouth in the dry season when river discharge is low. The estuary is described as hypersynchronous (Allen et al. 1980) because the tidal amplitude increases progressively towards the upper estuary, reaching a maximum of 2.8 m about 30 km away from the estuary mouth, before decaying in the fluvial sections (Olivry 1986). Numerous tidal creeks cut through the mangrove platforms and connect the mangrove forest to the

open water of the estuary (Fantong et al. 2016; Ndondo et al. 2021; Atekwana et al. 2022). The mean salinity of water in the Wouri Estuary is ~25 psu (Gabche and Smith 2002; Din et al. 2002). The salinity of the tidal creeks and that of the open estuary show variations influenced by tidal behavior, and because of seawater-freshwater mixing (Bessack et al. 2021; Atekwana et al. 2022).

3. Methodology

3.1 Sampling locations

I investigated the open water of the Wouri Estuary and Wouri River (N03°52'00.9", E009°31'55.9" to N04°07'02.3", E009°41'47.1") and the lower reaches of the of the Mungo River (N03°59'19.8", E009°38'08.5" to N04°07'21.1", E009°33'13.0") and the lower reaches of the Dibamba River (N03°54'49.9", E009°38'55.4" to N04°00'0.5", E009°50'54.4") (Fig. 1). I conducted my investigation in July 2023 during the peak of the rainy season and during high tide. The survey of the open estuary and the lower portion of the Wouri River was conducted at 18 sampling stations at ~2 to 3 km intervals along a 38 km transect on July 7th, 2023. Sampling began at the mouth of the estuary and the traverse was designed to intersect the flood tide-freshwater boundary in the upper estuary. River sampling was conducted at high tide at sampling intervals of ~2 to 3 km for 14 stations for the Mungo River on July 11th, 2023, and for 13 stations at intervals of ~2 to 3 Km for the Dibamba River on July 19th, 2023. For the river sampling, the first station was located in the open water of the estuary and sampling proceeded upstream along the river for 28 km for the Mungo River and 32 km for the Dibamba River.

3.2 Water sampling and sample processing

Grab samples for chemical and isotopic analyses were collected at 25 cm depth. Samples for the determination of DIC concentrations and the $\delta^{13}C_{DIC}$ were collected using a plastic syringe and injected through 0.45 µM syringe filters into pre-evacuated 50 mL glass vials pre-loaded with 1.5

mL of 85% phosphoric acid and magnetic stir bars. At each sampling station, 1 L polyethylene (PET) bottles were pre-rinsed thoroughly with the water to be sampled before collecting samples. The collected samples were later (within 6 h) filtered through 0.45 μM nylon into unacidified 30 mL PET bottles for the analyses of $\delta^{18}O$, silica, and nitrate. The lids of PET bottles were sealed with electrical tape to prevent accidental opening and evaporation during storage. All the water samples were kept cool and out of light and then transported to the University of California Davis, USA where they were kept in a refrigerator at 4°C.

3.3 Water sample analyses

At each sampling station, the water temperature, dissolved oxygen (DO), salinity, and pH were measured in situ at 25 cm depth below the water surface using a Hanna (HI98194) multi-parameter probe. Probe readings were recorded after the pH, temperature, and electrical conductivity stabilized. Water clarity was measured by lowering a Secchi disk into the water at each sampling location and noting the depth at disk extinction.

Alkalinity measurements were made by acid titration with 0.16 N sulfuric acid (Hach Company 1992) from filtered aliquots of the sample obtained from the 1 L PET bottles. Nitrate concentrations were measured by ion chromatography (Dionex ICS-6000). Silica concentrations were measured by spectrophotometry (CHEMetrics V-3000 series). Analysis for $\delta^{18}O$ was done using a Cavity Ringdown Spectrometer (PICARRO Isotope water analyzer L2140-i). DIC was quantified using the gas evolution extraction technique (Atekwana and Krishnamurthy 1998) and the $\delta^{13}C_{DIC}$ was measured on a Micromass Optima gas source isotope ratio mass spectrometer. All the isotopic ratios are reported in delta notation (δ) in per mil (‰). The $\delta^{18}O$ is reported relative to VSMOW standard and the $\delta^{13}C$ is reported relative to VPDB standard. The $\delta^{18}O$ and the $\delta^{13}C$ have a precision of better than 0.1‰.

4. Results

The results of temperature, water clarity, DO, salinity, $\delta^{18}O$, pH, alkalinity, DIC, $\delta^{13}C_{DIC}$, silica, and nitrate for the Wouri Estuary and Wouri River are presented in Table 1, for the Mungo River in Table 2, and for the Dibamba River in Table 3. In describing the axial variations of the different parameters across the open water of the Wouri estuary, the estuary mouth is assigned 0 km and distances progress towards the estuary head and Wouri River. I consider stations 0-10 km as the lower estuary, 10-20 km as the mid-estuary, and 20-38 km as the upper estuary and river. During the survey, the high tide front was crossed in the upper estuary at about 23 km from the estuary mouth. For the river surveys, high tide was crossed at 6 and 7 km from the mouths of the Mungo River and the Dibamba River, respectively.

4.1 Spatial variations in temperature, clarity, DO, salinity, and $\delta^{18}O$

The water temperature for the Wouri Estuary and Wouri River ranged from 26.4 to 28.8 °C and averaged 27.4 ±0.1°C. The water temperature increased from the mouth of the estuary towards the mid-estuary, decreased, and was nearly constant in the mid-estuary before decreasing and remaining constant in the upper estuary and Wouri River (Fig. 2a). The water temperature in the Mungo River ranged from 26.5 to 30°C and averaged 27.1 ±0.1°C. The water temperature in the Dibamba River ranged from 27.2 to 28.4 °C and averaged 27.6 ±0.1°C. The water temperature for the Mungo River and Dibamba River decreased from the mouth of the rivers towards the upstream (Table 2; Table 3).

In the Wouri Estuary and Wouri River, water clarity ranged from 44 to 142 cm and averaged 76 ±2 cm (Table 1). Water clarity, which was high and ranged between 100-142 cm in the lower estuary decreased continuously in the upper estuary and Wouri River, where it remained nearly constant at 50 cm (Fig. 2b). The clarity of the water in the Mungo River ranged from 30 to 102 cm and

averaged 60.6 ±2 cm. The clarity of the water in the Dibamba River ranged from 20 to 110 cm and averaged 68.6 ± 2cm. The clarity of the water for both the Mungo River and Dibamba River decreased from the mouth of the river towards the upstream (Table 2; Table 3).

In the Wouri Estuary and Wouri River, the DO concentrations ranged from 5.5 to 6.9 mg/L and averaged 6.3 ±1.5 mg/L. The DO concentrations were nearly constant around 7 mg/L throughout the lower estuary, then decreased to a minimum of ~6.0 mg/L in the mid-estuary and gradually increased to 7 mg/L in the upper estuary and the Wouri River (Fig. 2c). The DO concentrations in the Mungo River ranged from 6.3 to 7.6 mg/L and averaged 7.0 ±1.5 mg/L. The DO concentrations in the Dibamba River ranged from 5.7 to 7.3 mg/L and averaged 6.6 ±1.5 mg/L. The DO concentrations for the Mungo River and Dibamba River decreased from the mouth of the rivers towards the upstream (Table 2; Table 3).

The salinity in the Wouri Estuary and Wouri River averaged 12.8 ±0.01 psu and ranged from 0.02 to 38.8 psu. The salinity decreased continuously from 38.8 psu at the mouth of the estuary through the mid-estuary to a low of 0.2 psu in the mid-estuary and remained low through the upper estuary and the Wouri River (Fig. 2d). The salinity in the Mungo River ranged from 0.1 to 4.5 psu and averaged 1.1 ±0.01 psu. The salinity in the Dibamba River ranged from 0.1 to 6.2 psu and averaged 0.8 ±0.01psu. The salinity for the Mungo River and Dibamba River decreased from the mouth of the river towards the upstream (Table 2; Table 3).

The $\delta^{18}O$ of the Wouri Estuary and Wouri River ranged from -3.8 to -1.0 ‰ and averaged -2.8 ±0.3 ‰. The $\delta^{18}O$ decreased continuously from -1.0 ‰ in the lower estuary through the mid-estuary and stayed nearly constant at -3.8 ‰ in the upper estuary and Wouri River (Fig. 2e). The $\delta^{18}O$ in the Mungo River ranged from -4.9 to -3.7 ‰ and averaged -4.9 ±0.3 ‰. The $\delta^{18}O$ in the Dibamba River ranged from -4.0 to -2.5 ‰ and averaged -3.3 ±0.3 ‰. The $\delta^{18}O$ for both the Mungo River

and Dibamba River decreased from the mouth of the river towards the upstream (Table 2; Table 3).

4.2 Spatial variations of pH, alkalinity, DIC, $\delta^{13}C_{DIC}$

In the Wouri Estuary and Wouri River, the pH ranged from 6.5 to 7.8 and averaged 7.2 ±0.02. The pH decreased slowly from 7.8 in the lower estuary to 7.2 in the mid-estuary, then increased to 7.5 in the upper estuary before decreasing to 7.2 at the estuary head (Fig. 3a). The pH in the Mungo River ranged from 6.8 to 7.1 and averaged 6.9 ±0.02. The pH in the Dibamba River ranged from 6.4 to 7.0 and averaged 6.7 ±0.02. The pH for both the Mungo River and Dibamba River decreased from the mouth of the rivers towards the upstream (Table 2; Table 3).

The average alkalinity concentration in the Wouri Estuary and Wouri River was 28 ±1 mg/L (as $CaCO_3$) and ranged from 12 to 60 mg/L. Alkalinity concentrations generally decreased from 60 mg/L in the lower estuary to 20 mg/L mid-estuary and stayed nearly constant in the upper estuary and Wouri River (Fig. 3b). The alkalinity concentrations in the Mungo River ranged from 21.2 to 24.4 mg/L and averaged 23.1 ±1 mg/L. The alkalinity concentrations in the Dibamba River ranged from 7 to 20.8 mg/L and averaged 10.8 ±1 mg/L. The alkalinity concentrations for both the Mungo River and Dibamba River decreased from the mouth of the rivers towards the upstream (Table 2; Table 3).

The DIC concentrations in the Wouri Estuary and Wouri River averaged 7.3 ±0.1 mg C/L and ranged from 3.3 to 13.8 mg C/L. The DIC concentration which was 13.8 mg C/L in the lower estuary decreased to 5 mg C/L in the mid-estuary and remained nearly constant through the upper estuary and Wouri River (Fig. 3c). The DIC concentrations in the Mungo River ranged from 5.2 to 9.9 mg C/L and averaged 5.1 ±0.1 mg C/L. The DIC concentrations in the Dibamba River ranged from 0.8 to 1.5 mg C/L and averaged 1.1 ±0.1 mg C/L. The DIC concentrations for both the Mungo

River and Dibamba River decreased from the mouth of the rivers towards the upstream (Table 2; Table 3).

In the Wouri Estuary and Wouri River, the $\delta^{13}C_{DIC}$ ranged from -17.6 to -3.1 ‰ and averaged -11.2 ±0.1 ‰. The $\delta^{13}C_{DIC}$ decreased slowly from -3.1 to -4.8 ‰ in the lower estuary, and then steeply to -17.6 ‰ in the upper estuary before increasing slightly to -15.6 ‰ in the Wouri River (Fig. 3d). The $\delta^{13}C_{DIC}$ in the Mungo River ranged from -15.0 to -12.3 ‰ and averaged -14.0 ±0.1 ‰. The $\delta^{13}C_{DIC}$ in the Dibamba River ranged from -19.8 to -16.9 ‰ and averaged -18.6 ±0.1 ‰. The $\delta^{13}C_{DIC}$ for the Mungo River and Dibamba River decreased from the mouth of the rivers towards the watershed (Table 2; Table 3).

4.3 Spatial variation of silica and nitrate

Silica concentrations in the Wouri Estuary and Wouri River ranged from 3.7 to 13.5 mg/L and averaged 9.8 ±1.5 mg/L. The silica concentrations increased from 3.7 mg/L in the lower estuary to the mid estuary where the silica concentrations fluctuated between 12.0 to 13.7 mg/L in the upper estuary and Wouri River (Fig. 4a). The silica concentrations for the Mungo River averaged 16.4 ±1.5 mg/L and ranged from 10.1 mg/L in the estuary to 19.4 mg/L (Table 2). The silica concentrations for the Dibamba River averaged 8.4 ±1.5 mg/L and ranged from 5.2 to 10.12 mg/L (Table 3). The silica concentrations increased progressively upstream for both the Mungo River and Dibamba River.

In the Wouri Estuary and Wouri River, the nitrate concentrations varied between 0.01 to 26.61 mg/L and averaged 7.88 ±1.5 mg/L. The nitrate concentration increased from 14.8 mg/L in the lower estuary to 21.2 mg/L in the mid-estuary before decreasing to 4.2 mg/L in the mid-estuary (Fig. 4b). The nitrate concentrations then increased to 5.3 mg/L in the mid estuary and decreased to 0.1 mg/L and stayed low in the upper estuary and Wouri River (Fig. 4b). The nitrate

concentrations for the Mungo River averaged 6.1 ±1.5 mg/L and ranged from 0.04 to 11.18 mg/L (Table 2). The nitrate concentrations for the Dibamba River averaged 3.77 ±1.5 mg/L and ranged from 0.53 to 9.26 mg/L (Table 3). The nitrate concentrations were generally higher for river stations near the river mouth and decreased upstream in both the Mungo River and the Dibamba River.

5. Discussion

5.1 Axial variations of the physical and chemical parameters in the open water of the Wouri Estuary

The axial trends in water temperature (Fig. 2a), salinity (Fig. 2d), and $\delta^{18}O$ (Fig. 2e) which generally decrease from the mouth of the estuary towards the estuary head become nearly constant after the high tide front was crossed. The alkalinity (Fig. 3b) and DIC (Fig. 3c) concentrations and the $\delta^{13}C_{DIC}$ (Fig. 3d) also decreased from the estuary mouth towards the estuary head and changed very little after I crossed the high tide front. Silica showed a continuous increase in concentration from the estuary mouth towards the head and changed very little after the high tide front was crossed (Fig. 4a). In contrast, nitrate had higher concentrations in the lower estuary, which decreased towards the estuary head, and stayed low and nearly constant after I crossed the high tide front (Fig. 4b). I test if the spatial distribution of our measured parameters can be explained using a seawater-freshwater mixing model.

5.2Hydrologic mixing in the open water of the Wouri Estuary

Salinity and $\delta^{18}O$ are conservative and are therefore good tracers of mixing between seawater and freshwater (Lewis 1980; Fry 2002). Freshwater input into the Wouri Estuary is from the Wouri River at the estuary head, the Mungo River, and the Dibamba River which discharge into the

estuary at ~15 km from the estuary mouth (Fig. 1). The freshwater endmember for salinity is held constant at 0 psu for the Wouri River, the Mungo River and the Dibamba River. The freshwater $\delta^{18}O$ was determined by averaging the $\delta^{18}O$ values of the three most upstream stations in the Wouri River, Mungo River, and Dibamba River with salinities of 0 psu (Table 1: Table 2: Table 3) and presented in Table 4. Because I did not measure the salinity and $\delta^{18}O$ values for the seawater endmember, I initially assumed a $\delta^{18}O$ value of 0 ‰. Additionally, I assumed a salinity of 39 psu which was the salinity measured for my most seaward station during the survey. My mixing relationships using the salinity of 39 psu and a $\delta^{18}O$ value of 0 ‰. for the seawater endmember failed to describe the salinity-$\delta^{18}O$ relationship for the open estuary and the Wouri River, the Mungo River, or the Dibamba River.

I conducted a least squares regression for the salinity-$\delta^{18}O$ data for the open estuary and the Wouri River which is positive and strongly correlated ($\delta^{18}O = 0.068$ salinity- 3.7; $R^2 = 0.97$), indicating a two-endmember mixing between seawater and freshwater (Lewis 1980; Loder 1985; Fry 2002; Xie and Wu 2023). The intercept of the regression equation to the $\delta^{18}O$ axis at a salinity of 0 psu is identical to the average $\delta^{18}O$ of -3.7 ‰ estimated for the Wouri River endmember (Table 4). However, if I assume a $\delta^{18}O$ of 0 ‰ for the seawater endmember, then the salinity estimated from the regression equation is 54 psu, which is much higher than I measured and much higher than 33-37 psu reported for the Atlantic Ocean (Berger et al. 2014; Da-Allada et al. 2014; Dovlo 2016; Nyadjro et al. 2022). Nevertheless, using a $\delta^{18}O$ river endmember of -3.7, -4.6, and -2.9 ‰ for the Wouri River, Mungo River, and Dibamba River, respectively, and a seawater endmember $\delta^{18}O$ 0 ‰ and salinity of 54 psu (Table 4) I constructed hydrologic mixing lines for seawater and the three rivers (Fig. 5). The data from my axial survey of the open water of the Wouri Estuary and Wouri River lie along the salinity-$\delta^{18}O$ hydrologic mixing for seawater and freshwater. Furthermore, data

from the Mungo River and Dibamba River do not fall along the seawater-open water of the estuary-Wouri River mixing line. The salinity-$\delta^{18}O$ relationship for the Mungo River has a more negative $\delta^{18}O$ and a lower slope (0.055), while the Dibamba River has a more positive $\delta^{18}O$ endmember (Table 4) and a higher slope (0.087) compared to the Wouri River-seawater endmember relationship (Fig. 5). The more negative $\delta^{18}O$ for the Mungo River is consistent with higher elevations in the mountainous catchment where the higher altitudes cause greater depletion in the $\delta^{18}O$ (Clark and Fritz 2013). The topography of the Dibamba watershed is low and rainout of the air mass moving into the terrestrial interior controls the isotopic composition of the rain and stream water in the watershed (Clark and Fritz 2013). The $\delta^{18}O$ for the Wouri River shows that tributaries of the Wouri River collect water from both mountainous areas to the west and non-mountainous regions to the east.

I infer from the positive correlation between salinity and $\delta^{18}O$ in our axial survey (Fig. 5) that in spite of freshwater discharge from the Mungo River and the Dibamba Rivers occurring mid-estuary, I can characterize the hydrologic mixing by the Wouri River endmember. The Wouri River, Mungo River, and Dibamba River discharge 40 x 10^6 m^3/d, 60 x 10^6 m^3/d, and 40 x 10^6 m^3/d, respectively, into the Wouri Estuary (Gabehe and Smith 2002). Yet the $\delta^{18}O$ of the river endmembers indicate minimal contribution of discharge from the Mungo River and the Dibamba River to the open estuary during our survey. Although it appears paradoxical, I attribute this lack of mixing of the Mungo River and the Dibamba River to my axial sampling along seawater-Wouri River, different sampling dates for the Mungo and Dibamba Rivers, and tidal advance down the Mungo River and Dibamba River. Additionally, my experiment in the Mungo River and Dibamba River was focused on obtaining the freshwater $\delta^{18}O$ endmembers that would allow me to

characterize the contribution of the major rivers to mixing in the mid-to-lower estuary during my survey and to elucidate if these rivers were sources of nutrients to the estuary.

5.3 Nutrients in the open water of the Wouri Estuary

Determining the sources of nutrients and their fate in estuaries is critical to elucidate the role of nutrient perturbation on carbon cycling (Fry 2002; Borges and Gynpens 2010; Cotovicz et al. 2021). The Mungo River, Wouri River, and Dibamba River watersheds and the Atlantic Ocean are sources of nutrients and solutes delivered into the Wouri Estuary (Angwe and Gabche 1997; Gabche and Smith 2002; Baok 2007; Atangana 2013; Ngoran 2016; Fomenky et al. 2019). I measured high nitrate concentrations (up to 21.61 mg/L) in the open water of the Wouri Estuary (Table 1; Fig. 4b). However, the concentrations of nitrate in the surface water of the Atlantic Ocean over the past 10 years are low, and average 0.045 mg/L (Global Ocean Biogeochemistry Analysis and Forecast 2023), thus revealing that seawater is not the source of the high nitrate in the Wouri Estuary. Terrestrial and anthropogenic sources of nitrate in the Wouri Estuary include point sources from plantations and nonpoint sources from subsistence farming in the Mungo River, Wouri River, and Dibamba River watersheds. Additionally, improper disposal of sewage and waste from small towns in the Mungo River, Wouri River, and Dibamba River watersheds and improper disposal of domestic and industrial waste in the city of Douala are possible sources of nitrate (Gabche and Smith 2002; Atangana 2013; Ngoran 2016; Fomenky et al. 2019; Mbusnum et al. 2020). The nitrate concentrations measured in the Mungo River, Wouri River, and Dibamba River range between 0.04 to 11.18 mg/L, with lower concentrations at the mouths of these rivers (Table 2; Table 3). Therefore, to elucidate if the source of the nitrate in the estuary is terrestrial, I need to follow a terrestrial tracer delivered into the estuary and assess its mixing behavior. I contend that I should observe a coupled behavior of the terrestrial tracer with nitrate if nitrate delivered from

land is conserved in hydrologic mixing or observe a decay behavior over space if nitrate is utilized by phytoplankton or diluted by hydrologic mixing. Silica is a geogenic solute that can be used to trace the source and fate of nutrients in estuarine systems (Livingstone 1963; DeMaster 1981; Bell 1994). The salinity-silica relationship for the open water of the estuary and the Wouri River (Fig. 6a) is negatively correlated (Wouri Estuary: silica = -0.23 salinity + 12.82, $R^2 = 0.96$) indicating a two-end member mixing. The salinity-silica relationships show higher silica concentrations from the Mungo River watershed and lower silica concentrations for the Dibamba River watershed compared to the silica concentration from the Wouri River watershed (Fig. 6a). Similar to the salinity-$\delta^{18}O$ behavior (Fig. 5), there are clear differences in the watershed signatures for silica (Fig. 6a). Additionally, because silica concentrations from the Mungo River and Dibamba River do not cluster around the freshwater endmember of the salinity-silica relationship (Fig. 6a), I infer that the Mungo River and Dibamba River are not contributing silica to the open water of the Wouri Estuary during our survey.

I trace the source of anthropogenic nitrate pollution in the Wouri Estuary by assessing the mixing behavior between salinity and nitrate (Fig. 6b), which is relatively poor (Nitrate =0.43 salinity +2.41; $R^2 = 0.62$). This poor relationship between salinity and nitrate is used to suggest that nitrate pollution in the open water of the Wouri Estuary is not from a seawater or freshwater source. I support my contention that nitrate pollution is not from the watersheds because of the lower nitrate concentrations in the Wouri River, Mungo River, and Dibamba River (Table 1; Table 2; Table 3; Fig. 6b). Additionally, the nitrate concentrations are lower compared to higher concentrations observed in the lower portion of the Wouri Estuary. Moreover, if the source of nitrate was terrestrial, I would expect to observe progressively lower nitrate concentrations towards the estuary

mouth because of dilution by seawater and utilization by phytoplankton. Thus, the nitrate pollution in the open water of the Wouri Estuary appears to be in situ in the lower portion of the estuary.

5.4 Dissolved inorganic carbon in the open water of the Wouri Estuary

Two endmembers mixing between salinity and alkalinity and between salinity and DIC provide a means for assessing the sources and distribution of DIC in estuaries (e.g., Stumn and Morgan 1993; Fry 2002). DIC concentrations and the $\delta^{13}C_{DIC}$ in aqueous systems are controlled by CO_2 input, carbonate dissolution and precipitation reactions, heterotrophic microbial respiration of organic matter, photosynthesis by phytoplankton, aquatic DIC exchange with atmospheric CO_2 or from mixing of carbon from different pools (Cai and Wang 1998; Borges and Gypens 2010; Cotovicz 2019, 2021). Therefore, the processes that add or remove carbon from the estuarine DIC pool will cause changes in the DIC concentrations and the $\delta^{13}C_{DIC}$, thus forming the basis for using salinity and DIC parameters to model carbon mixing and processing (e.g., Sackett Moore 1966; Strain and Tan 1979; Spiker, 1980; Coffin and Cifuentes, 1999; Hellings et al.1999; Fry 2002). A two-endmember mixing relationship between salinity and alkalinity (Fig. 7a) is positively correlated (Alkalinity = 1.1Salinity + 13.8; R^2=0.96). A similar two-endmember mixing relationship (Fig. 7b) is observed between salinity and DIC concentrations (DIC = 0.24Salinity + 4.2; R^2=0.94). The salinity-alkalinity and salinity-DIC relationship indicates a seawater source for alkalinity and DIC in the Wouri Estuary because of higher concentrations compared to freshwater sources (Table 1; Table 2; Table 3). I interpret the positive correlation between salinity and alkalinity and between salinity and DIC to result from seawater-freshwater hydrologic mixing. The alkalinity and DIC concentrations in the Mungo River are higher and those for the Dibamba River are lower compared to those of the freshwater endmember in the salinity-alkalinity (Fig. 7a) or salinity-DIC relationships (Fig. 7b) for the open water of the Wouri Estuary and Wouri River.

5.5 Carbon cycling in the open water of the Wouri Estuary

The conservative mixing behavior of salinity-DIC-$\delta^{13}C_{DIC}$ is a critical tool to elucidate the processes that control DIC cycling in estuarine systems (Strain and Tan 1979; Peterson et al. 1994; Hellings et al. 1999). A three-endmember relationship between salinity, DIC concentration, and the $\delta^{13}C_{DIC}$ offers a robust approach to assessing carbon cycling beyond tidal controlled hydrologic mixing, and I use the approach of Fry (2002). Salinity in estuaries is conserved (e.g., Fig. 5) and the relationship between salinity and alkalinity (Fig. 7a) and salinity and DIC concentrations (Fig. 7b) allows me to use a single freshwater endmember for mixing in the open water of the Wouri Estuary, in spite of multiple freshwater sources. The choices for my seawater endmember and the freshwater endmember for salinity, DIC concentration, and $\delta^{13}C_{DIC}$ are presented in Table 5. The model behavior based on my selected seawater and freshwater endmember properties is shown in Fig. 8 as a blue dashed line (Line 1). The $\delta^{13}C_{DIC}$ in the upper and mid-estuary deviated from our model line slightly when the salinity <15 psu and markedly in the mid to lower estuary when the salinity >15 psu (Fig. 8). I developed another conservative mixing model to fit our data by iteration which is shown as Model Line 2 in Figure 8. To fit my data with model 2, I needed a seawater endmember with a salinity of 70 psu which is unlikely, because salinities measured in the Atlantic Ocean range from 33 to 37 psu (Berger et al. 2014; Da-Allada et al. 2014; Dovlo 2016; Nyadjro et al. 2022). The main reason why data from the Wouri Estuary does not fit Model 1 is that the $\delta^{13}C_{DIC}$ is much lower than predicted by the conservative mixing relationship in the mid to lower estuary, indicating that there are additional processes controlling carbon cycling in the water column (Strain and Tan 1979; Peterson et al. 1994; Hellings et at. 1999).

Deviations from salinity-DIC-$\delta^{13}C_{DIC}$ mixing curves that show $\delta^{13}C_{DIC}$ data below the conservative mixing curves have been previously reported (Coffin and Cifuentes 1999; Bouillon

et al. 2003; Bouillon et al. 2011). Such deviations are attributed to respiration of organic matter that adds CO_2 depleted in ^{13}C which causes depletion of the $\delta^{13}C$ of the DIC (Bouillon et al. 2003; Bouillon et al. 2011). In the Wouri Estuary, the location where the $\delta^{13}C_{DIC}$ is lower than predicted by the salinity-DIC-$\delta^{13}C_{DIC}$ model is in the mid to lower estuary with salinities greater than 15 psu. The respiration of terrestrially derived organic matter can explain the addition of CO_2 depleted in ^{13}C in the DIC pool. The $\delta^{13}C_{DIC}$ for the portion of the estuary dominated by freshwater is up to -16.7 ‰ (Fig. 3d), which I use to suggest that the organic matter brought into the estuary from the watersheds is from C-3 vegetation (Ludwig 1996; Dittmar et al.2001; Lamb et al. 2006; Liu et al.2007), and consistent with measured $\delta^{13}C$ values of dissolved organic carbon as low as -30.0‰ in the watersheds of Nyong River east of the Wouri Estuary in Cameroon (Nkoue and Ndondo 2008). Additionally, marine-dominated regions of estuaries exhibit higher $\delta^{13}C_{DIC}$ in the water column that ranges from -3 to -7‰ (Fig. 3c) resulting from the predominance of seawater DIC (Mook and Tan 1991; Chanton and Lewis 1999). I infer that the respiration of organic matter fueled by higher nitrate concentrations is the likely cause for the depleted $\delta^{13}C_{DIC}$ in the mid to lower estuary (Fig. 8). The oxidation of the organic matter, in turn, causes the nonconservative response to the salinity-DIC-$\delta^{13}C_{DIC}$ relationship (Cifuentes et al. 1988; Giresse and Cahet 1997; Fry 2002; Bouillon et al. 2003; Cai et al. 2004; Bouillon et al. 2011 Cotovicz et al.2015,2021; Dutta and Choudhury 2021; Hee et al. 2023). I suggest that the nitrate that fuels the respiration of organic matter in the lower Wouri Estuary is from anthropogenic input related to the direct release of untreated sewage by ships destined for the Douala seaport but anchored in waiting in the lower estuary. Additionally, I suggest that the untreated sewage contributes to the organic matter that is oxidized in the lower estuary in situ. I surmise that anthropogenic perturbations of the cycling of

carbon in the Wouri Estuary which occurs in the mid to lower estuary is not from the watershed influx of nutrients or nutrients from anthropogenic activities in the city of Douala.

6. Conclusions

The physical, chemical, and stable carbon isotopic composition water collected axially across the open water of a tropical mangrove estuary and from three rivers that feed the estuary were used to characterize the key processes driving carbon cycling. A salinity-$\delta^{18}O$ mixing model a during high tide survey depicts mixing between seawater and a single freshwater endmember in the open water of the estuary. Nitrate concentrations (up to 21.61 mg/L) recorded in the lower estuary were significantly higher than in rivers that feed the estuary and seawater that mixes with freshwater in the estuary. A salinity-silica relationship which traced the geogenic silica from the terrestrial watershed allowed me to suggest that a poor salinity-nitrate mixing relationship means that nitrate pollution of the lower estuary is in situ. I attribute the in-situ pollution of the lower estuary with nitrate to ships anchored in waiting to offload or pick up cargo at the seaport located at the estuary head. A salinity-alkalinity and salinity-DIC mixing models indicate two-endmember mixing consistent with tidal controlled hydrologic mixing. However, a salinity-DIC-$\delta^{13}C_{DIC}$ conservative model failed to characterize carbon cycling in the lower estuary. The poor fit to the salinity-DIC-$\delta^{13}C_{DIC}$ conservative model occurred because of lower-than-expected $\delta^{13}C_{DIC}$ in the lower estuary, which was driven by isotopically light CO_2 input into the water column from nitrate-induced heterotrophic organic matter respiration. I suggest that anthropogenic pollution by nitrate drives carbon cycling in the lower reaches of this tropical mangrove estuary.

Funding

This study was funded by the US National Science Foundation (NSF) grant from the Office of International Science and Engineering (OISE) - Grant #1827065 and #1827072.

References

Abril G, Nogueira M, Etcheber H, Cabeçadas G, Lemaire E, Brogueira MJ (2002) Behaviour of organic carbon in nine contrasting European estuaries. Estuarine, coastal and shelf science 54(2):241-62

Abril G, Borges AV (2005) Carbon dioxide and methane emissions from estuaries. In Greenhouse gas emissions—fluxes and processes: hydroelectric reservoirs and natural environments. Berlin, Heidelberg: Springer Berlin Heidelberg pp.187-207

Ajonina G, Diamé A, Kairo J (2008) Current status and conservation of mangroves in Africa: An overview. World Rainforest Movement Bulletin 133:1-6

Ako AA, Eyong GE, Shimada J, Koike K, Hosono T, Ichiyanagi K, Richard A, Tandia BK, Nkeng GE, Roger NN (2014) Nitrate contamination of groundwater in two areas of the Cameroon Volcanic Line (Banana Plain and Mount Cameroon area). Applied Water Science 4:99-113

Allen GP, Salomon JC, Bassoullet, P, Du Penhoat Y, De Grandpre C (1980) Effects of tides on mixing and suspended sediment transport in macro tidal estuaries. Sedimentary Geology 26 (1–3): 69–90

Angwe CA, Gabche CE1 (1997) Quantitative estimation of land-based sources of pollution to the coastal and marine environment of the Republic of Cameroon. Research Center for Fisheries and Oceanography, Limbe, Cameroon pp. 33

Atekwana EA, Ramatlapeng GJ, Ali HN, Njilah IK, Ndondo GR (2022) Tide-salinity patterns reveal seawater-freshwater mixing behavior at a river mouth and tidal creeks in a tropical mangrove estuary. Journal of African Earth Sciences 196:104684

Atekwana EA, Tedesco LP, Jackson LR (2003) Dissolved inorganic carbon (DIC) and hydrologic mixing in a subtropical riverine estuary, southwest Florida, USA. Estuaries 26:1391-400

Atekwana EA, Krishnamurthy RV (1998) Seasonal variations of dissolved inorganic carbon and $\delta^{13}C$ of surface waters: application of a modified gas evolution technique. Journal of Hydrology 205(3-4):265-78

Atangana A (2013) A generic assessment of waste disposal at Douala City practice, principles and uncertainties (Doctoral dissertation, University of the Free State).

Baok G (2007) Pollution des eaux de rivière et les impacts biologiques sur les populations riveraines: cas de la rivière Mgoua dans la zone industrielle de Douala-Bassa (Cameroun). Mémoire Master of Science en Gestion de l'Eau, Université de Dschang

Berger H, Treguier AM, Perenne N, Talandier C (2014) Dynamical contribution to sea surface salinity variations in the eastern Gulf of Guinea based on numerical modelling. Climate Dynamics 43(11):3105-22

Bell RG (1994) Behaviour of dissolved silica, and estuarine/coastal mixing and exchange processes at Tairua Harbour, New Zealand. New Zealand. Journal of Marine and Freshwater Research 28(1):55-68

Besack F, Rodrigue ES, Nwutih AG, Dieudonné ER, Willy SE, Brice N, Junior ME, Michel-Remi HT, Raphael O, Minette TE (2021) Spatial and Temporal Variation of the Hydrological Parameters in the Wouri-Nkam Section of the Cameroon Estuary, Central African Atlantic Coast. Open Journal of Marine Science 11(4):129-56

Borges AV (2005) Do we have enough pieces of the jigsaw to integrate CO_2 fluxes in the coastal ocean? Estuaries 28:3-27

Borges AV, Gypensb N (2010) Carbonate chemistry in the coastal zone responds more strongly to eutrophication than ocean acidification. Limnology and Oceanography 55(1):346-53

Borges AV, Abril G (2011) Carbon dioxide and methane dynamics in estuaries. In: Wolanski E, McLusky D. (Eds.), Treatise on Estuarine and Coastal Science. Academic Press, Amsterdam, pp. 119–161

Bouillon S, Frankignoulle M, Dehairs F, Velimirov B, Eiler A, Abril G, Etcheber H, Borges AV (2003) Inorganic and organic carbon biogeochemistry in the Gautami Godavari estuary (Andhra Pradesh, India) during pre-monsoon: The local impact of extensive mangrove forests. Global biogeochemical cycles 17(4):1114

Bouillon S, Dehairs F, Schiettecatte LS, Borges AV 2007. Biogeochemistry of the Tana estuary and delta (northern Kenya). Limnology and Oceanography 52(1):46-59

Bouillon S, Connolly RM, Gillikin DP. 7.07 (2011) Use of stable isotopes to understand food webs and ecosystem functioning in estuaries. Treatise on Estuarine and Coastal Science 7:143-173

Cai WJ, Wang Y (1998) The chemistry, fluxes, and sources of carbon dioxide in the estuarine waters of the Satilla and Altamaha Rivers, Georgia. Limnology and Oceanography 43(4):657-68

Cai WJ, Dai M, Wang Y, Zhai W, Huang T, Chen S, Zhang F, Chen Z, Wang Z (2004) The biogeochemistry of inorganic carbon and nutrients in the Pearl River estuary and the adjacent Northern South China Sea. Continental Shelf Research. 24(12):1301-19

Chanton JP, Lewis FG (1999) Plankton and dissolved inorganic carbon isotopic composition in a river-dominated estuary: Apalachicola Bay, Florida. Estuaries 22:575-83

Chen CT, Huang TH, Fu YH, Bai Y, He X (2012) Strong sources of CO_2 in upper estuaries become sinks of CO_2 in large river plumes. Current Opinion in Environmental Sustainability 4(2):179-85

Chen CT, Huang TH, Chen YC, Bai Y, He X, Kang Y (2013) Air–sea exchanges of CO_2 in the world's coastal seas. Biogeosciences 10(10):6509-44

Cifuentes LA, Sharp JH, Fogel ML (1988) Stable carbon and nitrogen isotope biogeochemistry in the Delaware estuary. Limnology and Oceanography 33(5):1102-15

Clark ID, Fritz P (2013) Environmental isotopes in hydrogeology. CRC press.

Climate (Accessed 08 June 2023) (Cameroon). https://en.climate-data.org/africa/cameroon/littoral/douala-890444/.

Coffin RB, Cifuentes LA (1999) Stable isotope analysis of carbon cycling in the Perdido Estuary, Florida. Estuaries 917-26

Corcoran E, Ravilious C, Skuja M (2007) Mangroves of Western and Central Africa. hhtps://www.umep- wcmc.org/resources/publications/UNEP_WCMC_bio_series/26.htm.

Cotovicz LC, Ribeiro RP, Régis CR, Bernardes M, Sobrinho R, Vidal LO, Tremmel D, Knoppers BA, Abril G (2021) Greenhouse gas emissions (CO_2 and CH_4) and inorganic carbon behavior in an urban highly polluted tropical coastal lagoon (SE, Brazil). Environmental Science and Pollution Research 28:38173-92

Cotovicz Jr LC, Knoppers BA, Deirmendjian L, Abril G (2019) Sources and sinks of dissolved inorganic carbon in an urban tropical coastal bay revealed by δ13C-DIC signals. Estuarine, Coastal and Shelf Science 1220:185-95

Cotovicz LC, Knoppers BA, Brandini N, Costa Santos SJ, Abril G (2015) A strong CO_2 sink enhanced by eutrophication in a tropical coastal embayment (Guanabara Bay, Rio de Janeiro, Brazil). Biogeosciences 12(20):6125-46

Da-Allada CY, Du Penhoat Y, Jouanno J, Alory G, Hounkonnou NM (2014) Modeled mixed-layer salinity balance in the Gulf of Guinea: Seasonal and interannual variability. Ocean Dynamics 64:1783-802

DeMaster DJ (1981) The supply and accumulation of silica in the marine environment. Geochimica et Cosmochimica acta 45(10):1715-32

De Souza Machado AA (2017) Coastal pollution of aquatic systems: Literature review and experiments focusing on metal fate on estuaries (Doctoral dissertation, Queen Mary University of London).

Dittmar T, Lara RJ (2001) Driving forces behind nutrient and organic matter dynamics in a mangrove tidal creek in North Brazil. Estuarine, Coastal and Shelf Science 52(2):249-59

Dittmar T, Lara RJ, Kattner G (2001) River or mangrove? Tracing major organic matter sources in tropical Brazilian coastal waters. Marine Chemistry 73(3-4):253-71

Din N (2001) Mangroves du Cameroun : statut écologique et perspectives de gestion durable. Doctoral dissertation, Thèse de Doctorat d'Etat, Université de Yaoundé I, Cameroun

Din N, Priso RJ, Kenne M, Ngollo DE, Blasco F (2002) Early growth stages and natural regeneration of Avicennia germinans (L.) Stearn in the Wouri estuarine mangroves (Douala-Cameroon). Wetlands Ecology and Management. 10:461-72

Din N, Baltzer F (2008) Richesse Floristique et Evolution des mangroves de l'Estuaire du Cameroun. African Geosciences Review 2:119-30

Din N, Saenger P, Jules PR, Siegfried DD, Basco F (2008) Logging activities in mangrove forests: A case study of Douala Cameroon. African Journal of Environmental Science and Technology 2(2):022-30

Din N, Ngo-Massou VM, Essomè-Koum GL, Ndema-Nsombo E, Kottè-Mapoko E, Nyamsi-Moussian L (2017) Impact of urbanization on the evolution of mangrove ecosystems in the Wouri River Estuary (Douala Cameroon). Coastal wetlands: Alteration and remediation. 81-131

Diop ES, Gordon C, Semesi AK, Soumaré A, Diallo N, Guissé A, Diouf M, Ayivor JS (2002) Mangroves of Africa. In Mangrove ecosystems: Function and management Berlin, Heidelberg: Springer Berlin Heidelberg 63-121

Diop ES (1993) Conservation and sustainable utilization of mangrove forests in Latin America and Africa Regions. Okinawa (Japan): CIT0044 ISME. Part II Africa ISME/UNESCO Project Mangrove Ecosystems Technical Reports 3

Diop ES, Fabres J, Pravettoni R, Barusseau JP, Descamps C, Ducrotoy JP (2014) The western and central Africa land–sea interface: a vulnerable, threatened, and important coastal zone within a changing environment. The land/ocean interactions in the coastal zone of West and Central Africa 1-8

Donato DC, Kauffman JB, Murdiyarso D, Kurnianto S, Stidham M, Kanninen M (2011) Mangroves among the most carbon-rich forests in the tropics. Nature Geoscience 4(5):293-7

Dovlo EK (2016) Seasonal variations in temperature and salinity in the Gulf of Guinea. Journal of Aquaculture and Marine Biology 4(2):2-7

Dubinina EO, Kossova SA, Miroshnikov AY, Fyaizullina RV (2017) Isotope parameters (δD, $\delta^{18}O$) and sources of freshwater input to Kara Sea. Oceanology 57:31-40

Dutta S, Choudhury AK (2021) An assessment of the temporal alterations in the trophic status and habitat heterogeneity of the anthropogenically influenced Bhagirathi–Hooghly estuary in

reference to phytoplankton community and environmental variables. Environmental Science and Pollution Research 28(35):48681-705

Eyre B, Balls P (1999) A comparative study of nutrient behavior along the salinity gradient of tropical and temperate estuaries. Estuaries 22:313-26

Fantong WY, Kamtchueng BT, Ketchemen-Tandia B, Kuitcha D, Ndjama J, Fouepe AT, Takem GE, Issa, Wirmvem MJ, Djomou SL, Ako AA (2016) Variation of hydrogeochemical characteristics of water in surface flows, shallow wells, and boreholes in the coastal city of Douala (Cameroon). Hydrological Sciences Journal 61(16):2916-29

Fomenky NN, Tening AS, Asongwe GA, Mbene K, Nka-Folep FF (2019) Seasonal variations of some physico-chemical properties of water sources that feed Rivers Wouri and Meme of Cameroon. African Journal of Environmental Science and Technology 13(11):425-38

Fotsi YF, Brenon I, Pouvreau N, Ferret Y, Latapy A, Onguene R, Jombe D, Etame J (2023) Exploring tidal dynamics in the Wouri estuary, Cameroon. Continental Shelf Research 259:104982

Fotsi YF, Pouvreau N, Brenon I, Onguene R, Etame J (2019) Temporal (1948–2012) and dynamic evolution of the Wouri estuary coastline within the Gulf of Guinea. Journal of Marine Science and Engineering 7(10):343

Frankignoulle M, Abril G, Borges A, Bourge I, Canon C, Delille B, Libert E, Théate JM (1998) Carbon dioxide emission from European estuaries. Science 282(5388):434-6

Fry B (2002) Conservative mixing of stable isotopes across estuarine salinity gradients: a conceptual framework for monitoring watershed influences on downstream fisheries production. Estuaries (2):264-71

Fusi M, Beone GM, Suciu NA, Sacchi A, Trevisan M, Capri E, Daffonchio D, Din N, Dahdouh-Guebas F, Cannicci S (2016) Ecological status and sources of anthropogenic contaminants in mangroves of the Wouri River Estuary (Cameroon). Marine Pollution Bulletin 109(2):723-33

Gabehe CE, Smith VS (2002) Water, salt and nutrients budgets of two estuaries in the coastal zone of Cameroon. West African Journal of Applied Ecology 3(1):69-89

Global Ocean Biogeochemistry Analysis and Forecast. E.U. Copernicus Marine Service Information [Dataset]. Accessed through Resource Watch.ww.resourcewatch.org. Accessed 8 October 2023

Gazeau F, Smith SV, Gentili B, Frankignoulle M, Gattuso JP (2004) The European coastal zone: characterization and first assessment of ecosystem metabolism. Estuarine, Coastal and Shelf Science 60(4):673-94

Giresse P, Cahet G (1997) Organic fluxes of Cameroonian rivers into the Gulf of Guinea: a quantitative approach to biodegradation in estuary and plume. Oceanologica Acta. 20(6):837-49

HACH Company (1992) Digital Titrator Model 16900–01 Manual. HACH Company, Loveland, Colorado.

Hee YY, Weston K, Suratman S, Akhir MF, Latif MT, Valliyodan S (2023) Biogeochemical and physical drivers of hypoxia in a tropical embayment (Brunei Bay). Environmental Science and Pollution Research (24):65351-63

Hellings L, Dehairs F, Tackx M, Keppens E, Baeyens W (1999) Origin and fate of organic carbon in the freshwater part of the Scheldt Estuary as traced by stable carbon isotope composition. Biogeochemistry 47:167-86

Hou W, Sun S, Wang M, Gu B, Li X, Zhang C, Jia R (2020) Variations in stable carbon and nitrogen isotopes of particulate organic matter in surface waters of water-receiving area of Eastern Route of South-to-North Water Transfer Project, China. Environmental Science and Pollution Research 27:2805-18

Huang TH, Fu YH, Pan PY, Chen CT (2012) Fluvial carbon fluxes in tropical rivers. Current Opinion in Environmental Sustainability 4(2):162-9

Joesoef A, Kirchman DL, Sommerfield CK, Cai WJ (2017) Seasonal variability of the inorganic carbon system in a large coastal plain estuary. Biogeosciences 14(21):4949-63

Lamb AL, Wilson GP, Leng MJ (2006) A review of coastal palaeoclimate and relative sea-level reconstructions using δ13C and C/N ratios in organic material. Earth-Science Reviews 75(1-4):29-57

Liu KK, Kao SJ, Wen LS, Chen KL (2007) Carbon and nitrogen isotopic compositions of particulate organic matter and biogeochemical processes in the eutrophic Danshuei Estuary in northern Taiwan. Science of the Total Environment 382(1):103-20

Livingstone DR (1993) Biotechnology and pollution monitoring: use of molecular biomarkers in the aquatic environment. Journal of Chemical Technology & Biotechnology 57(3):195-211

Loder JW (1985) Physical Controls on Phytoplankton production at tidal fronts. In Proceedings of the 19th European Marine Biology Symposium, 1985 1985. Cambridge University Press 3-21

Ludwig W, Probst JL, Kempe S (1996) Predicting the oceanic input of organic carbon by continental erosion. Global Biogeochemical Cycles 10(1):23-41

Mbusnum KG, Malleret L, Deschamps P, Khabouchi I, Asia L, Lebarillier S, Menot G, Onguene R, Doumenq P (2020) Persistent organic pollutants in sediments of the Wouri Estuary

Mangrove, Cameroon: Levels, patterns and ecotoxicological significance. Marine Pollution Bulletin 160:111542

Mook WG (1991) Stable carbon isotopes in rivers and estuaries. SCOPE 42, Biogeochemistry of Major World Rivers.

Naidoo G (2023) The mangroves of Africa: A review. Marine Pollution Bulletin 190:114859

Ndondo GR, Boum SN, Song F, Eyong GE, Komba DE, Nlend B, Etame J (2021) Hydrogeochemical Characteristics and Quality Assessment of Surface Water in an Agricultural Area in Equatorial Africa: The Mungo River Basin, Southwest Cameroon, Central Africa. Journal of Geoscience and Environnent Protection 9(03):164

Ndongo B, Mbouendeu SL, Tirmou AA, Njila RN, Dalle JD (2015) Tendances pluviométriques et impact de la marée sur le drainage en zone d'estuaire : cas du Wouri au Cameroun. Afrique Science : Revue Internationale des Sciences et Technologie 11(2):173-82

Nfotabong-Atheull A, Din N, Essomè Koum LG, Satyanarayana B, Koedam N, Dahdouh-Guebas F (2011) Assessing forest products usage and local residents' perception of environmental changes in peri-urban and rural mangroves of Cameroon, Central Africa. Journal of Ethnobiology and Ethnomedicine 7(1):1-3

Ngoran SD, Xue X, Ndah AB (2016) Exploring the challenges of implementing integrated coastal management and achieving sustainability within the Cameroon coastline. Revista de Gestão Costeira Integrada-Journal of Integrated Coastal Zone Management 16(1):45-56

Nkoue N, Gustave R.(2008) The carbon cycle in wet tropical domain: example of the forested Nyong river basin in the south Cameroon.

Nyadjro ES, Foli BA, Agyekum KA, Wiafe G, Tsei S (2022) Seasonal variability of Sea Surface salinity in the NW Gulf of Guinea from SMAP satellite. Remote Sensing in Earth Systems Sciences 5:83

Olivry JC (1986) Fleuves et rivières du Cameroun. Monographies hydrologiques ORSTOM pp. 733

Onguene R, Pemha E, Lyard F, Du-Penhoat Y, Nkoue G, Duhaut T, Njeugna E, Marsaleix P, Mbiake R, Jombe S, Allain D (2015) Overview of tide characteristics in Cameroon coastal areas using recent observations. Open Journal of Marine Science 5(01):81-98

Palit K, Rath S, Chatterjee S, Das S (2022) Microbial diversity and ecological interactions of microorganisms in the mangrove ecosystem: Threats, vulnerability, and adaptations. Environmental Science and Pollution Research 29(22): 32467-512

Peel MC, Finlayson BL, McMahon TA (2007) Updated world map of the Köppen-Geiger climate classification. Hydrology and Earth System Sciences 11(5):1633-44

Peterson B, Fry B, Hullar M, Saupe S, Wright R (1994) The distribution and stable carbon isotopic composition of dissolved organic carbon in estuaries. Estuaries 17:111-21

Ramatlapeng GJ, Atekwana EA, Ali HN, Njilah IK, Ndondo GR (2021) Assessing salinization of coastal groundwater by tidal action: The tropical Wouri Estuary, Douala, Cameroon. Journal of Hydrology: Regional Studies. 36:100842

Simon LN, Raffaelli D (2012) Assessing ecosystem effects of small–scale cutting of Cameroon mangrove forests. Journal of Ecology and Natural Environment 4(5):126-34

Sackett WM, Moore WS (1966) Isotopic variations of dissolved inorganic carbon. Chemical Geology 1:323-8

Strain PM, Tan FC (1979) Carbon and oxygen isotope ratios in the Saguenay Fjord and the St Lawrence Estuary and their implications for paleoenvironmental studies. Estuarine and Coastal Marine Science 8(2):119-26

Spiker E (1980) The behavior of ^{14}C and ^{13}C in estuarine water: effects of in situ CO2 production and atmospheric exchange. Radiocarbon 22(3):647-54

Stumm W, Morgan JJ, Drever JI (1993) Aquatic Chemistry, 2nd edition. John Wiley, New York.

Tide for fish chart of the Littoral region of Cameroon coast https://tides4fishing.com Wouri estuary. Wikipedia: en.wikipedia.org/wiki/Wouri_estuary. Accessed July 07, 2023

Twilley RR (1985) The exchange of organic carbon in basin mangrove forests in a southwest Florida estuary. Estuarine, Coastal and Shelf Science 20(5):543-57

Weather forecast map of Douala. https://www.weather-forecast.com/maps/Cameroon?hr=3 . Accessed July 07 2023

Xie R, Zhen L, Wu X, Li J (2023) Isotopic compositions (δD, $\delta^{18}O$) and end-member mixing for the control interface in a complex tidal region. Science of The Total Environment 866:161438

Zhang Y, Yang P, Yang H, Tan L, Guo Q, Zhao G, Li L, Gao Y, Tong C (2019) Plot-scale spatiotemporal variations of CO_2 concentration and flux across water–air interfaces at aquaculture shrimp ponds in a subtropical estuary. Environmental Science and Pollution Research 26:5623-37

Tables

Table 1 : Global positioning satellite (GPS) locations, temperature (Temp), dissolved oxygen (DO), water clarity, salinity, stable oxygen isotope ($\delta^{18}O$), pH, alkalinity, dissolved inorganic carbon (DIC), stable isotopic composition of carbon of DIC ($\delta^{13}C_{DIC}$), Silica and nitrate for the Wouri Estuary and Wouri River.

Sample ID	GPS reading		Temp	DO	Clarity	Salinity	$\delta^{18}O$	pH	Alkalinity	DIC	$\delta^{13}C$	Silica	Nitrate
	Latitude	Longitude	°C	ppm	cm	psu	‰	S.U.	mg/L	mg C/L	‰	mg/L	mg/L
WR1	N03°52'00.9"	E009°31'55.9"	27.62	6.58	102	38.81	-1.1	7.76	60	13.77	-3.1	3.7	13.80
WR2	N03°52'58.3"	E009°32'59.7"	27.51	6.74	145	34.94	-1.9	7.77	44.2	11.41	-5.6	6.2	11.72
WR3	N03°53'48.1"	E009°34'37.7"	27.76	6.82	135	31.15	-1.6	7.66	49.5	12.64	-5.1	5.4	17.04
WR4	N03°54'44.6"	E009°34'12.9"	28.08	6.7	98	28.35	-1.7	7.59	48.4	9.10	-5.3	6.1	20.50
WR5	N03°55'37.8"	E009°34'46.7"	28.11	6.62	108	29	-1.6	7.59	48.2	12.15	-4.9	5.5	19.02
WR6	N03°56'30.7"	E009°35'23.0"	28.36	6.72	102	23.51	-2.0	7.5	41.6	10.64	-6.0	7.1	10.22
WR7	N03°57'23.1"	E009°35'59.9"	28.35	6.85	88	19.65	-2.1	7.37	40.1	9.06	-7.2	7.0	8.58
WR8	N03°58'17.2"	E009°36'38.4"	28.12	6.75	79	11.64	-2.7	7.27	29.6	8.17	-9.6	8.8	21.61
WR9	N03°59'08.2"	E009°37'17.0"	27.41	6.14	57	6.24	-3.3	7.01	21.1	5.06	-12.9	11.9	2.50
WR10	N03°59'57.3"	E009°37'57.5"	27.04	6.03	53	3.69	-3.4	6.91	19.7	5.56	-14.3	11.9	7.75
WR11	N04°00'45.5"	E009°38'44.4"	27.26	5.55	44	1.97	-3.6	6.96	18.2	3.68	-15.6	12.5	6.19
WR12	N04°01'31.7"	E009°39'25.1"	27.18	5.49	46	0.52	-3.7	7.21	15.2	5.25	-15.6	13.3	2.69
WR13	N04°02'22.2"	E009°40'07.3"	27.11	5.71	58	0.12	-3.8	7.34	14.2	4.30	-16.0	13.5	0.06
WR14	N04°03'06.9"	E009°41'04.7"	27.21	6.08	47	0.1	-3.7	7.4	13.5	4.59	-17.6	12.8	0.02
WR15	N04°03'53.5"	E009°41'33.8"	26.44	6.2	52	0.04	-3.8	7.17	12.1	3.39	-16.3	12.1	0.01
WR16	N04°04'57.3"	E009°41'29.2"	26.53	6.55	56	0.04	-3.7	6.8	11.6	4.13	-16.7	13.1	0.12
WR17	N04°05'59.4"	E009°41'35.0"	26.46	6.19	50	0.04	-3.7	6.51	11.6	4.04	-13.8	13.0	0.01
WR18	N04°07'02.3"	E009°41'47.1"	26.42	6.06	51	0.022	-3.8	6.45	11.7	4.29	-16.5	12.9	0.01

Table 2: Global positioning satellite (GPS) locations, temperature (Temp), dissolved oxygen (DO), water clarity, salinity, stable oxygen isotope ($\delta^{18}O$), pH, alkalinity, dissolved inorganic carbon (DIC), stable isotopic composition of carbon of DIC ($\delta^{13}C_{DIC}$), Silica and nitrate for the Mungo River.

Sample ID	GPS reading		Temp	DO	Clarity	Salinity	$\delta^{18}O$	pH	Alkalinity	DIC	$\delta^{13}C$	Silica	Nitrate
	Latitude	Longitude	ºC	ppm	cm	psu	‰	S.U.	mg/L	mg/C/L	‰	mg/L	mg/L
M1	N03°59'19.8"	E009°38'08.5"	27.84	7	36	4.51	-4.9	6.88	21.2	5.15	-13.6	11.4	9.63
M2	N03°59'41.3"	E009°33'09.4"	27.42	7.13	32	3.79	-4.5	6.94	22.8	6.62	-14.1	13.9	11.18
M3	N03°59'59.5"	E009°33'04.8"	27.34	7.6	42	2.6	-4.8	7.07	23.4	6.62	-15.1	12.1	4.02
M4	N04°00'48.4"	E009°33'29.8"	29.96	7.19	30	1.95	-	6.65	22.6	5.96	-12.3	13.6	5.27
M5	N04°01'07.5"	E009°33'36.1"	26.81	7.22	32	2.29	-3.7	6.78	22.3	4.98	-13.6	15.2	7.24
M6	N04°02'38.8"	E009°34'34.7"	26.57	6.3	52	0.14	-3.9	6.99	23	5.69	-13.2	16.2	-
M7	N04°03'12.4"	E009°34'42.5"	26.51	6.28	64	0.09	-4.7	6.84	22.6	5.16	-14.4	17.5	8.56
M8	N04°03'58.5"	N04°03'58.5"	26.59	6.67	70	0.07	-4.6	6.73	22.4	6.23	-14.5	16.6	8.66
M9	N04°04'48.7"	E009°35'04.4"	26.56	6.9	72	0.05	-4.3	6.84	23.1	6.25	-13.1	19.0	0.04
M10	N04°04'57.5"	E009°35'03.0"	26.56	6.68	73	0.06	-4.8	6.81	23	7.79	-13.1	17.3	9.88
M11	N04°05'08.0"	E009°35'07.6"	26.75	7.5	90	0.05	-5.2	6.85	24	6.35	-14.5	18.9	0.11
M12	N04°05'41.4"	E009°35'55.0"	26.73	7.23	82	0.06	-4.3	6.91	23.4	6.64	-14.9	19.1	3.77
M13	N04°06'17.4"	E009°33'11.8"	26.66	7.52	102	0.06	-4.7	6.9	24.4	9.94	-14.9	19.0	9.46
M14	N04°07'21.1"	E009°33'13.0"	26.8	7.45	71	0.06	-4.6	7	24	7.49	-15.0	19.4	2.05

- = not measured

Table 3: Global positioning satellite (GPS) locations, temperature (Temp), dissolved oxygen (DO), water clarity, salinity, stable oxygen isotope ($\delta^{18}O$), pH, alkalinity, dissolved inorganic carbon (DIC), stable isotopic composition of carbon of DIC ($\delta^{13}C_{DIC}$), Silica and nitrate for the Dibamba River.

Sample ID	GPS reading		Temp	DO	Clarity	Salinity	$\delta^{18}O$	pH	Alkalinity	DIC	$\delta^{13}C$	Silica	Nitrate
	Latitude	Longitude	ºC	ppm	m	psu	‰	S.U.	mg/L	mg/C/L	‰	mg/L	mg/L
D1	03°54'49.4"N	09°38'55.4"E	28.39	6.78	20	6.21	-3.8	6.38	20.8	-	-	7.3	4.91
D2	03°55'13"N	009°40'57.7"E	28.1	6.46	52	1.7	-2.8	6.73	15.4	4.15	-16.9	7.0	6.01
D3	03°55'58.5"N	09°42'12.3"E	27.99	6.27	52	1.65	-2.7	6.74	16.2	5.02	-	8.6	6.02
D4	03°56'19"N	09°43'41.5"E	27.8	5.98	48	0.42	-3.4	6.57	11.7	4.72	-19.3	7.8	4.78
D5	03°56'38.2"N	09°45'10.1"E	27.72	5.77	47	0.25	-3.4	6.9	14.2	5.03	-18.5	9.1	9.26
D6	03°57'38.8"N	09°46'0.3"E	27.66	6.12	41	0.07	-3.5	7	9.1	3.51	-19.8	8.8	0.53
D7	03°57'15.6"N	09°47'40.6"E	27.49	5.93	50	0.12	-3.5	6.81	8.7	4.14	-18.1	9.7	2.76
D8	03°56'47.6"N	09°49'44.5"E	27.56	6.38	85	0.03	-4.0	6.85	7.5	2.92	-19.0	9.8	3.09
D9	03°56'33.8"N	09°49'58.9"E	27.44	6.88	100	0.02	-3.8	6.72	7.3	2.75	-19.2	5.2	2.73
D10	03°57'19.2"N	09°51'25.5"E	26.38	7.1	87	0.02	-3.4	6.62	7.5	2.63	-18.5	8.6	1.00
D11	03°58'32.1"N	09°51'42.7"E	27.37	7.17	101	0.02	-2.5	6.4	7.0	2.79	-18.2	10.1	2.55
D12	03°59'42.9"N	09°51'35.7"E	27.23	7.13	99	0.02	-2.6	6.93	7.2	2.79	-19.3	7.8	2.55
D13	04°00'0.5"N	09°50'54.4"E	27.15	7.33	110	0.03	-3.7	6.52	7.4	2.83	-17.6	9.7	2.88

- = not measured

Table 4: Endmember values for salinity and the stable oxygen isotope of oxygen ($\delta^{18}O$) for seawater, the Wouri River, the Mungo River, and the Dibamba River.

	Salinity (psu)	$\delta^{18}O$ (‰)	
Seawater	52	0	
Wouri River	0	-3.7	
Mungo River	0	-4.6	
Dibamba River	0	-2.9	

Table 5: Endmember values for the dissolved inorganic carbon (DIC), stable carbon isotopic of DIC ($\delta^{13}C$), and salinity for seawater and freshwater (the Wouri River).

	Freshwater			Seawater		
	DIC (mmol/L)	$\delta^{13}C$ (‰)	Salinity (psu)	DIC (mmol/L)	$\delta^{13}C$ (‰)	Salinity (psu)
	C_R	$\delta^{13}C_R$	S_R	C_S	$\delta^{13}C_S$	S_S
Line 1	0.3	-18	0	1.2	0	52
Line 2	0.3	-18	0	1.2	0	70

Figures

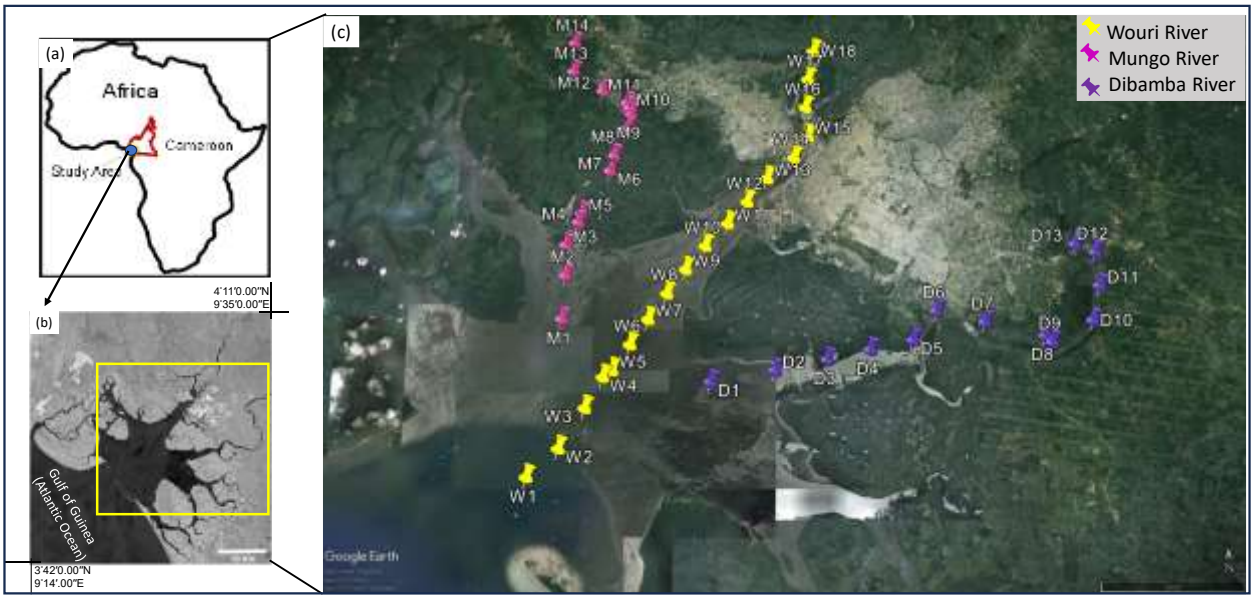

Figure 1 : (A) Location of the tropical Wouri Estuary in Douala Cameroon, (B) a radarsat image showing the Wouri Estuary, (C) A Google Earth map image showing the sampling stations across the axial transect of the open estuary and segments of the Mungo River

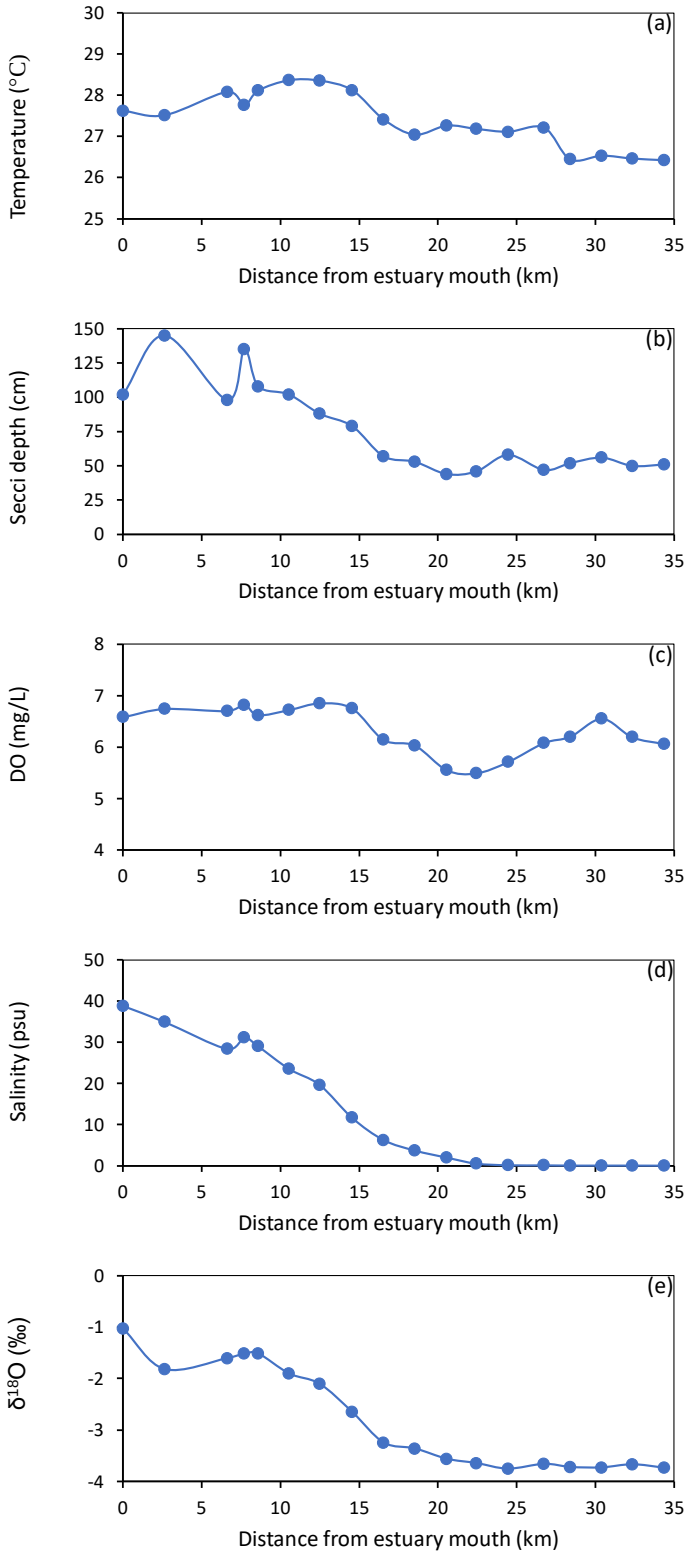

Figure 2: Spatial variations of (a) Temperature (b) Clarity (c) Dissolved Oxygen (d) Salinity (e) $\delta^{18}O$ from the mouth of the estuary (0km) to the estuary head (35km).

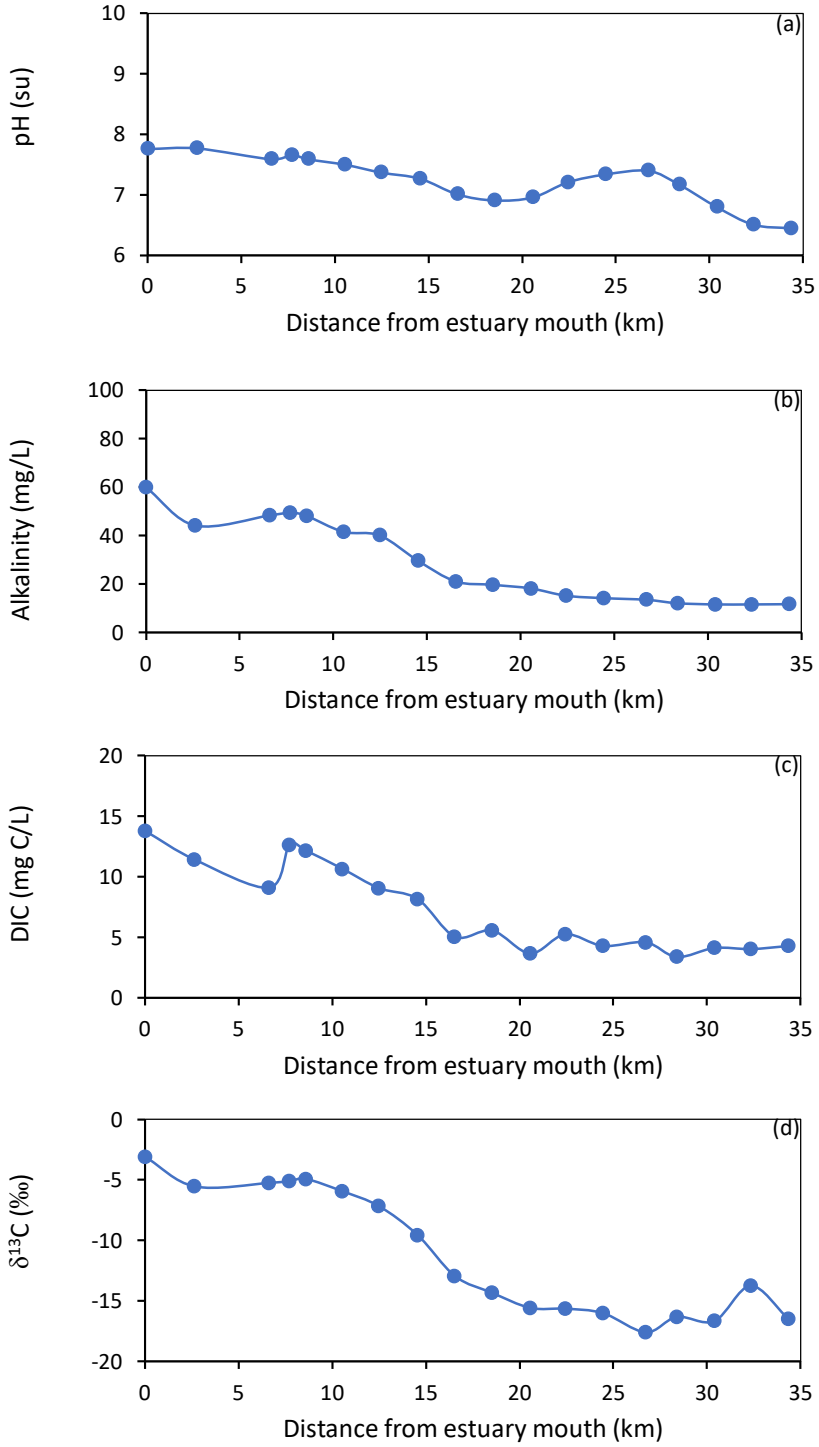

Figure 3: Spatial variations of (a) pH (b) Alkalinity (c) DIC(d) $\delta^{13}C$ from the mouth of the estuary (0km) to the estuary head (35km).

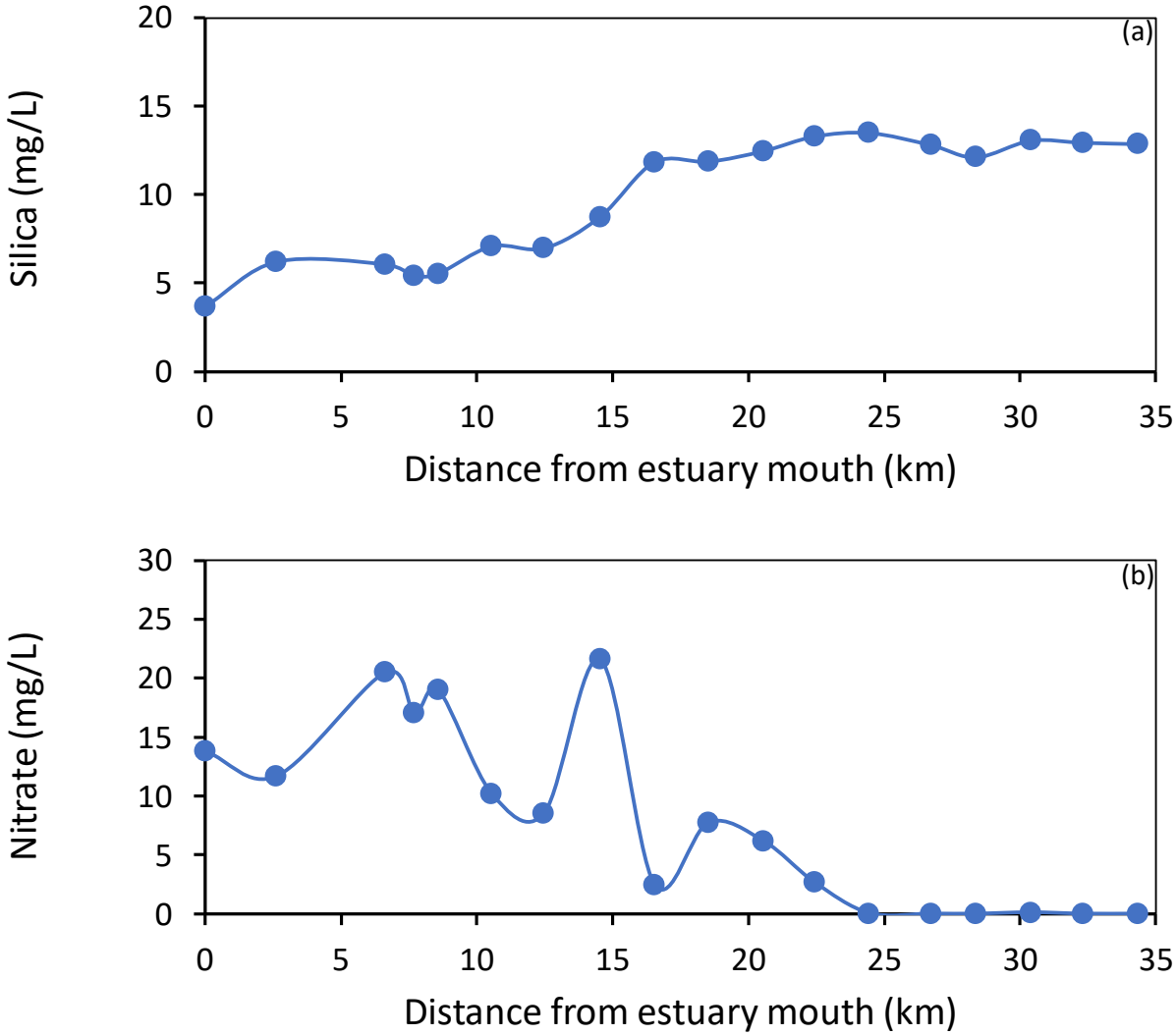

Figure 4: Spatial variations of (a) Silica and (b) Nitrates from the mouth of the estuary (0km) to the estuary head (35km).

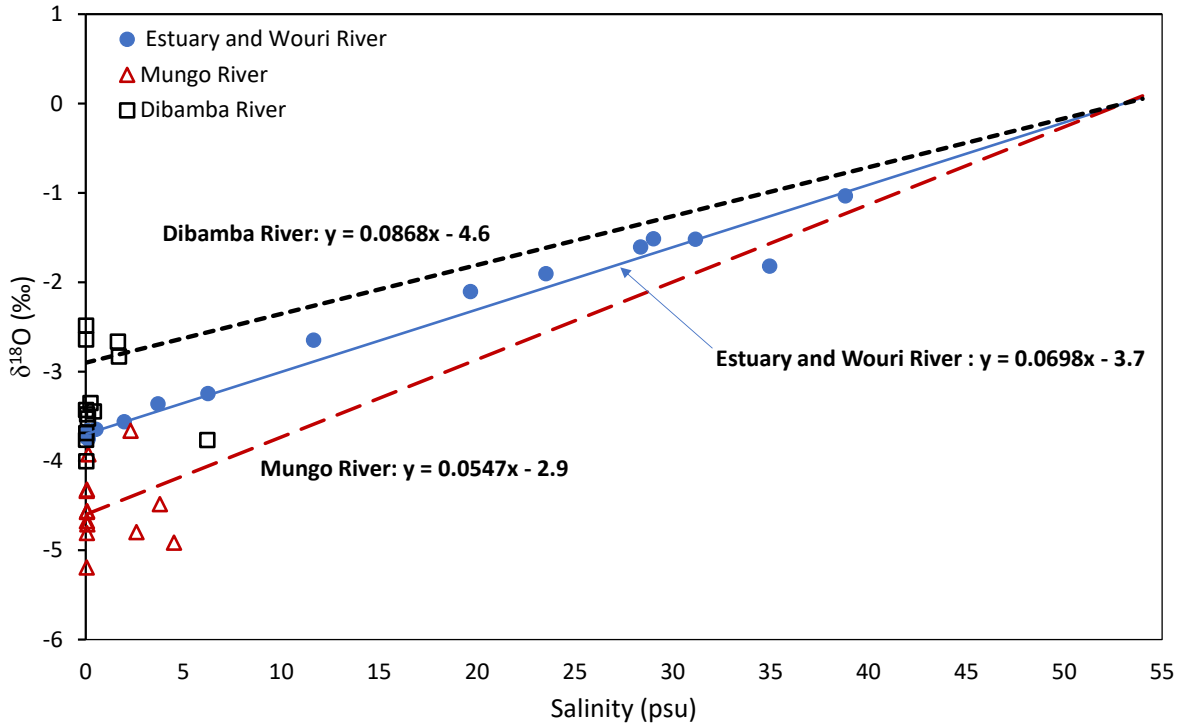

Figure 5: Seawater-freshwater hydrologic mixing relationship between salinity and $\delta^{18}O$ across the open water of the Wouri Estuary and the Wouri River, the Mungo River, and the Dibamba River.

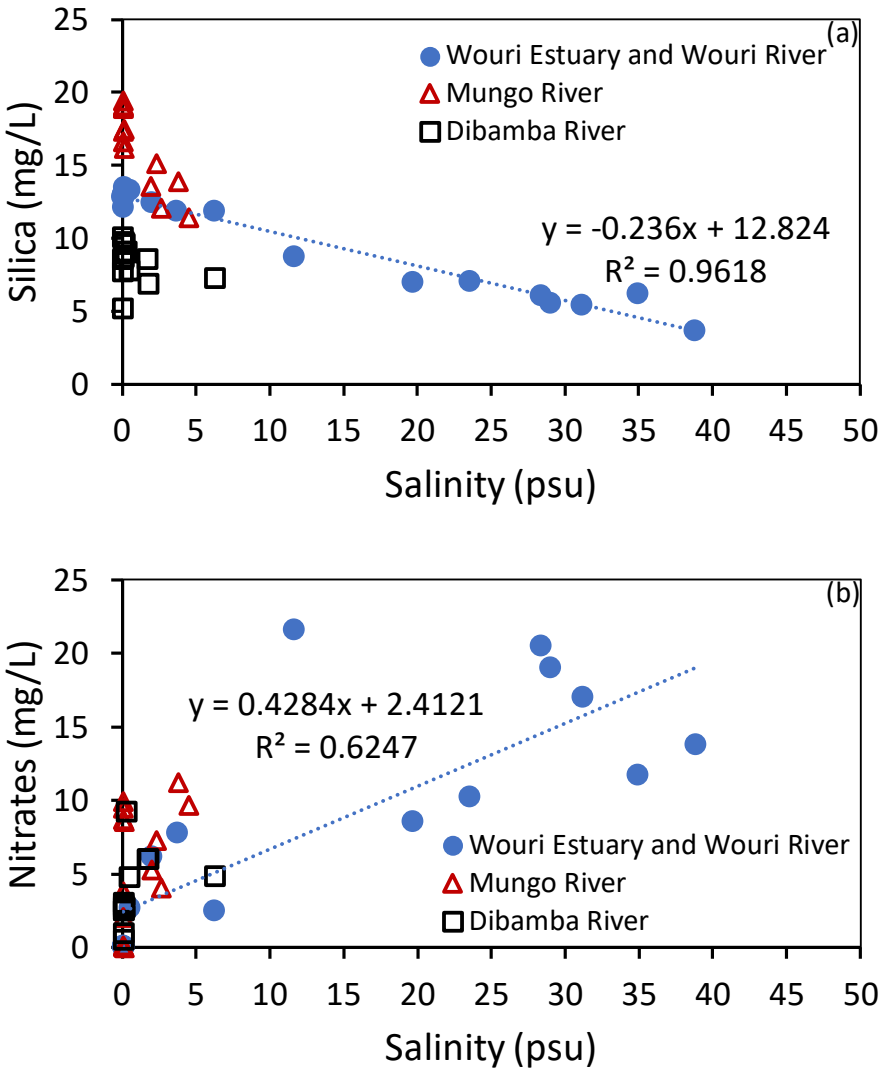

Figure 6: Plots of salinity variation as a function of (a) Silica and (b) Nitrates in the open water of the Wouri Estuary, and the segments of the Mungo River, and Dibamba River watersheds.

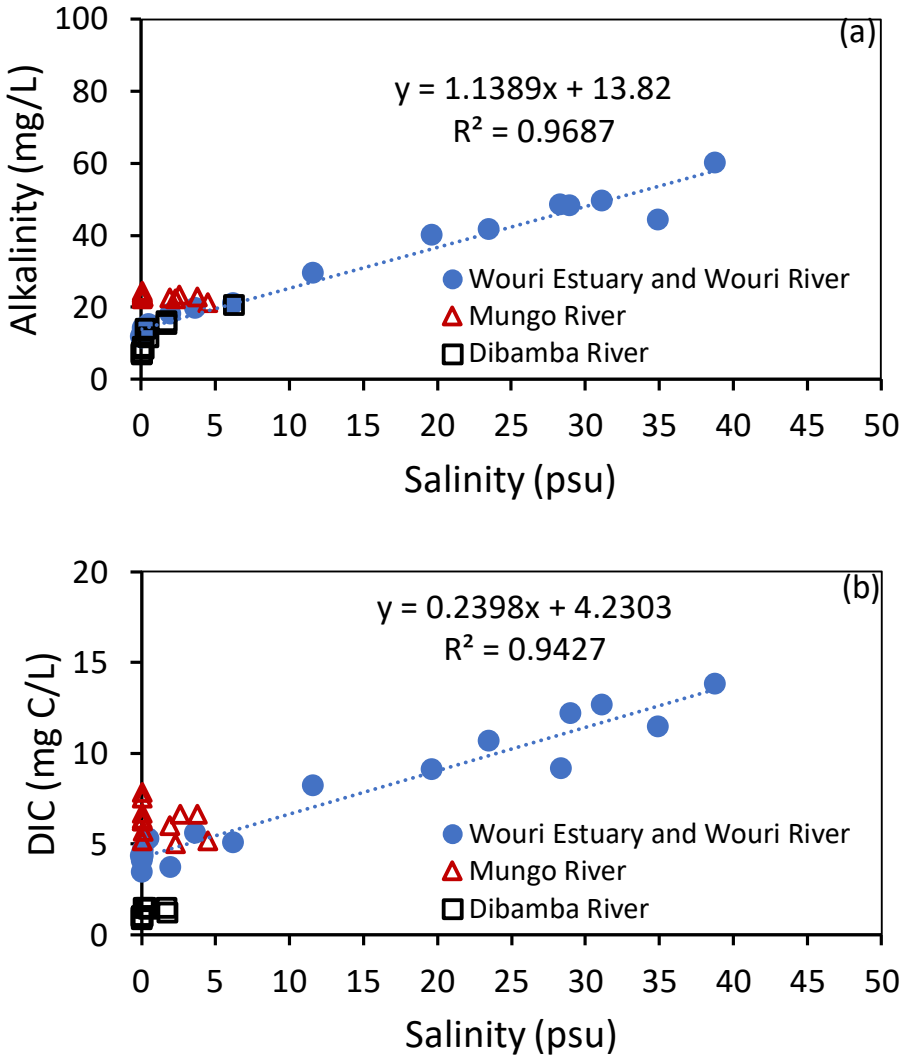

Figure 7: Plots of salinity variation as a function of (a) Alkalinity (b) DIC across the open water of the Wouri Estuary, and the segments of the Mungo River and Dibamba River watersheds.

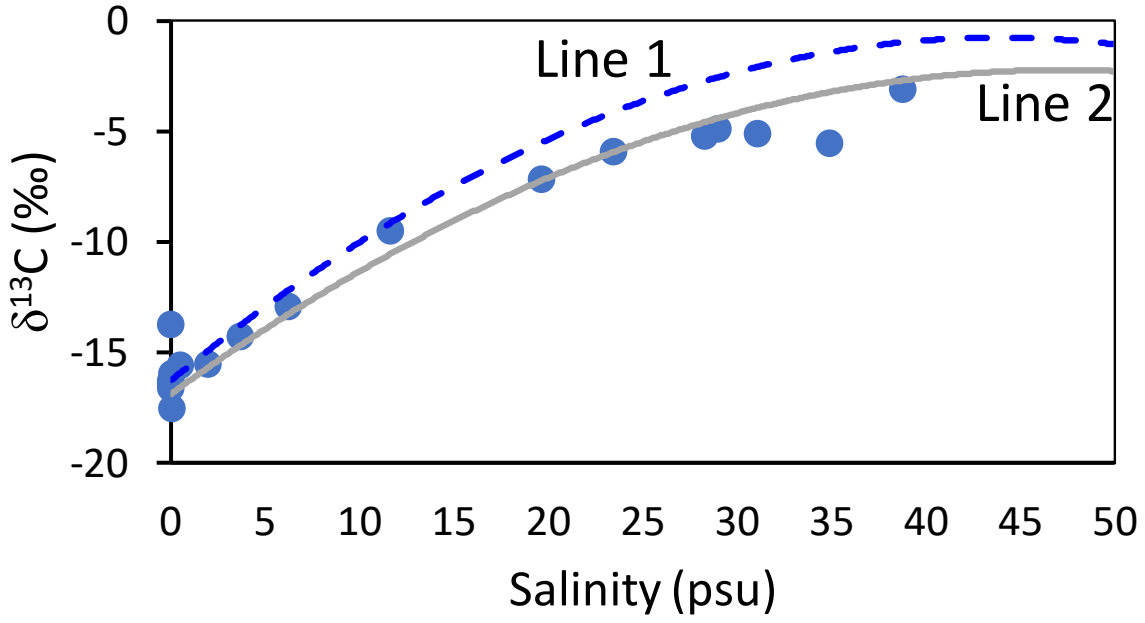

Figure 8: Plot of salinity vs. dissolved inorganic carbon and $\delta^{13}C$. A three-endmember mixing from two conservative mixing models (line 1 and line 2) of salinity, DIC, and $\delta^{13}C$. Closed blue circles represent data from the Wouri Estuary. Model Line 2 modified from Fry, B 2002 by iteration.